Simulation of carbon isotope discrimination of the terrestrial biosphere

N. S. Suits,[1] A. S. Denning,[1] J. A. Berry,[2] C. J. Still,[3] J. Kaduk,[4] J. B. Miller,[5,6] and I. T. Baker[1]

Received 29 August 2003; revised 31 March 2004; accepted 24 November 2004; published 5 March 2005.

[1] We introduce a multistage model of carbon isotope discrimination during C3 photosynthesis and global maps of C3/C4 plant ratios to an ecophysiological model of the terrestrial biosphere (SiB2) in order to predict the carbon isotope ratios of terrestrial plant carbon globally at a 1° resolution. The model is driven by observed meteorology from the European Centre for Medium-Range Weather Forecasts (ECMWF), constrained by satellite-derived Normalized Difference Vegetation Index (NDVI) and run for the years 1983–1993. Modeled mean annual C3 discrimination during this period is 19.2‰; total mean annual discrimination by the terrestrial biosphere (C3 and C4 plants) is 15.9‰. We test simulation results in three ways. First, we compare the modeled response of C3 discrimination to changes in physiological stress, including daily variations in vapor pressure deficit (vpd) and monthly variations in precipitation, to observed changes in discrimination inferred from Keeling plot intercepts. Second, we compare mean $\delta^{13}C$ ratios from selected biomes (Broadleaf, Temperate Broadleaf, Temperate Conifer, and Boreal) to the observed values from Keeling plots at these biomes. Third, we compare simulated zonal $\delta^{13}C$ ratios in the Northern Hemisphere (20°N to 60°N) to values predicted from high-frequency variations in measured atmospheric CO_2 and $\delta^{13}C$ from terrestrially dominated sites within the NOAA-Globalview flask network. The modeled response to changes in vapor pressure deficit compares favorably to observations. Simulated discrimination in tropical forests of the Amazon basin is less sensitive to changes in monthly precipitation than is suggested by some observations. Mean model $\delta^{13}C$ ratios for Broadleaf, Temperate Broadleaf, Temperate Conifer, and Boreal biomes compare well with the few measurements available; however, there is more variability in observations than in the simulation, and modeled $\delta^{13}C$ values for tropical forests are heavy relative to observations. Simulated zonal $\delta^{13}C$ ratios in the Northern Hemisphere capture patterns of zonal $\delta^{13}C$ inferred from atmospheric measurements better than previous investigations. Finally, there is still a need for additional constraints to verify that carbon isotope models behave as expected.

Citation: Suits, N. S., A. S. Denning, J. A. Berry, C. J. Still, J. Kaduk, J. B. Miller, and I. T. Baker (2005), Simulation of carbon isotope discrimination of the terrestrial biosphere, *Global Biogeochem. Cycles*, *19*, GB1017, doi:10.1029/2003GB002141.

1. Introduction

[2] Atmospheric CO_2 concentrations have been increasing for the past 150 years due to combustion of fossil fuels, manufacture of cement, and biomass burning. In the 1980s, this anthropogenic CO_2 was added to the atmosphere at a rate of approximately 5.4 ± 0.3 Pg-C/year; in the 1990s the rate was 6.3 ± 0.4 Pg-C/year [*Intergovernmental Panel on Climate Change* (*IPCC*), 2001]. However, over these same periods, atmospheric CO_2 only increased at rates of 3.3 ± 0.1 and 3.2 ± 0.1 Pg-C/year, respectively. Consequently, during this time, there were natural sinks for nearly half of the anthropogenically added CO_2. However, in spite of this knowledge of bulk changes in atmospheric CO_2, the spatial and temporal distribution of the sinks, partitioning of the fluxes into land and ocean components, and the processes involved are still uncertain.

[1]Department of Atmospheric Sciences, Colorado State University, Fort Collins, Colorado, USA.
[2]Department of Plant Biology, Carnegie Institution of Washington, Stanford University, Stanford, California, USA.
[3]Geography Department, University of California, Santa Barbara, California, USA.
[4]Department of Geography, University of Leicester, Leicester, England, UK.
[5]National Oceanic and Atmospheric Administration/CMDL, Boulder, Colorado, USA.
[6]Also at Institute for Arctic and Alpine Research, University of Colorado, Boulder, Colorado, USA.

Copyright 2005 by the American Geophysical Union.
0886-6236/05/2003GB002141$12.00

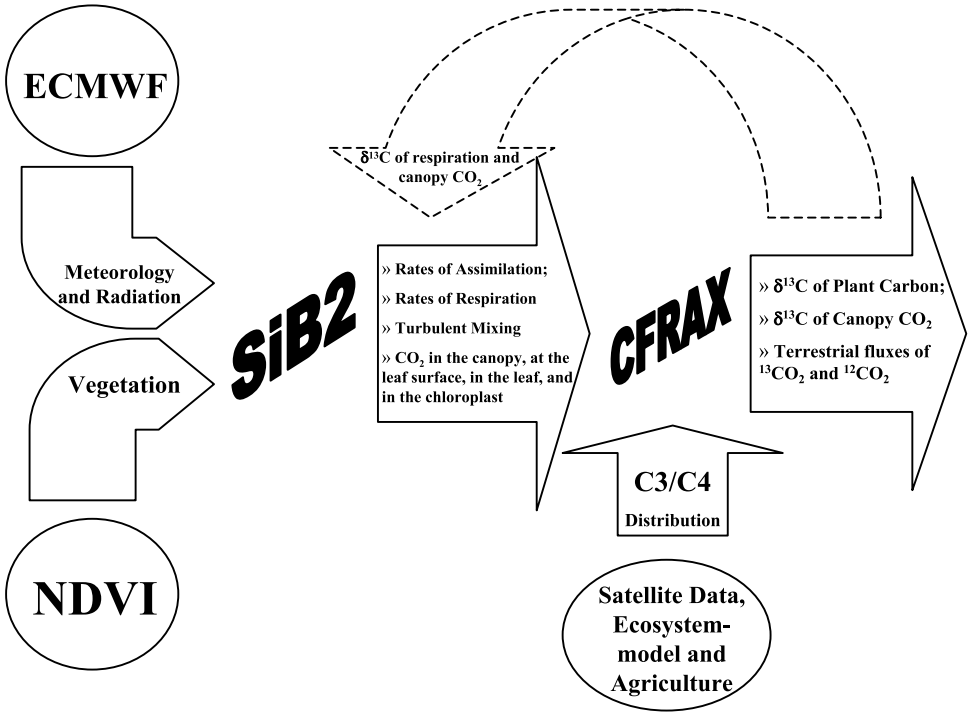

Figure 1. Flow of data in the simulation. ECMWF provides 6-hourly (1) wind speed at 10 m height, (2) temperature at 2 m, (3) relative humidity at 2 m, (4) total incident solar radiation, and (5) precipitation. Monthly vegetation maps (linearly interpolated each day) are from processed satellite data. C3/C4 plant distributions are from ecosystem modeling, satellite data, and maps of agriculture [*Still et al.*, 2003]. SiB2 calculates (1) rates of assimilation, (2) leaf boundary layer, stomatal and mesophyll conductance, and (3) CO_2 concentrations in the plant (C_s, C_i, C_c) and canopy (C_a). C3/C4 distributions are from ecosystem modeling, satellite data, and maps of agriculture [*Still et al.*, 2003] (see Figure 2 in this paper). CRAX calculates carbon isotope discrimination of C3 and C4 plants. The dashed arrow indicates that CFRAX can be coupled interactively with SiB2 to provide $\delta^{13}C$ of respiration and canopy CO_2 during each time step. That feature is not used in this study.

[3] Carbon isotopes can be helpful in investigations of the sink because they give information about both sources and processes of CO_2 exchange. At the local level, carbon isotopes are helpful in understanding (1) plant water use efficiency and the response of plants to changes in precipitation and relative humidity [*Farquhar and Richards*, 1984; *Farquhar et al.*, 1988; *Condon et al.*, 1993; *Hall et al.*, 1993; *Schulze et al.*, 1996, 1998; *Ekblad and Högberg*, 2001; *Bowling et al.*, 2002; *Ometto et al.*, 2002], (2) variation in light distribution and stand structure [*Berry et al.*, 1997; *Buchmann et al.*, 1997a, 1997b; *Le Roux et al.*, 2001], (3) recycling of respired CO_2 [*Keeling*, 1961; *Schleser and Jayasekera*, 1985; *Sternberg*, 1989; *Lloyd et al.*, 1996; *Sternberg et al.*, 1997], and (4) determining the relative contributions of photosynthesis and respiration to total net ecosystem exchange [*Yakir and Wang*, 1996; *Bowling et al.*, 2001]. At the global scale, carbon isotopes have been used to (1) determine spatial and temporal distribution of sources and sinks and, in some cases, determine partitioning of oceanic and terrestrial fluxes [*Francey*, 1985; *Keeling et al.*, 1989, 1995; *Francey et al.*, 1995; *Tans et al.*, 1993; *Ciais et al.*, 1995a, 1995b; *Enting et al.*, 1995; *Fung et al.*, 1997; *Rayner et al.*, 1999; *Bousquet et al.*, 1999a, 1999b] and (2) to examine relative contributions of C3 and C4 plants to total primary productivity [*Lloyd and Farquhar*, 1994; *Ehleringer et al.*, 1997; *Sage et al.*, 1999]. Many of these studies show that plant discrimination can change rapidly and that it is very sensitive to environmental changes; however, most of the global models must make simplifying assumptions concerning carbon isotope discrimination of the terrestrial biosphere, and few models function on multiple spatial and temporal scales, so that the results can be directly compared to observations at both flux towers and flask stations.

[4] Previous studies that modeled carbon isotope discrimination of the terrestrial biosphere used monthly mean values of temperature, precipitation, and humidity, were driven by meteorology produced in a GCM, or were produced using modeled vegetation [*Lloyd and Farquhar*, 1994; *Fung et al.*, 1997; *Kaplan et al.*, 2002], and none operate within the framework of GCM which is simultaneously calculating turbulent exchange of heat, water, and carbon fluxes between the biosphere and atmosphere. We wanted to construct a model that was capable of being driven by observed meteorology and vegetation so that results could be compared to historical records. We also wanted a model that could function online with a GCM so that we could examine systematic relationships between

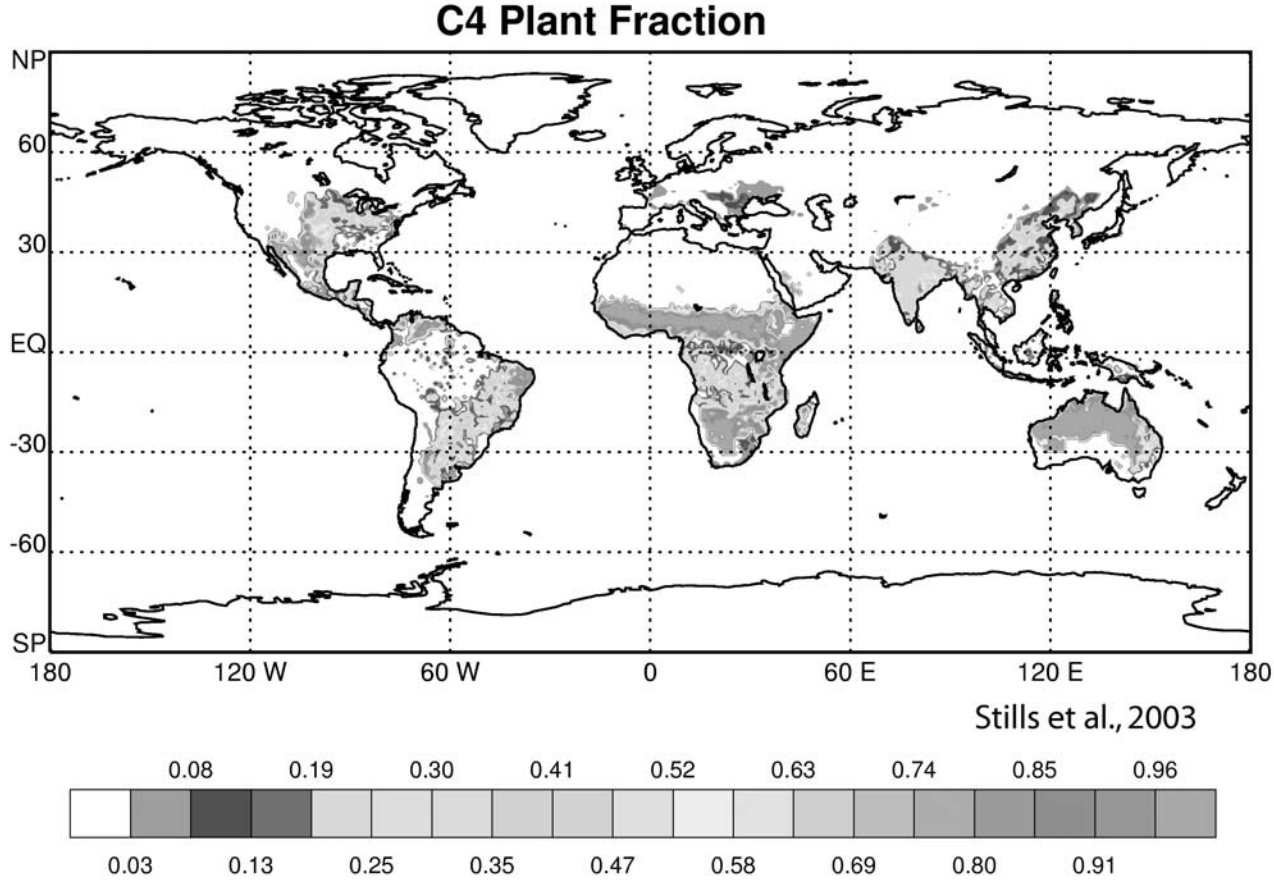

Figure 2. Distribution of C3 and C4 plants [*Still et al.*, 2003] is determined using remote sensing products [*Defries and Townshend*, 1994; *DeFries et al.*, 1998, 1999a, 1999b, 2000], physiological modeling [*Collatz et al.*, 1998], crop fraction maps [*Ramankutty and Foley*, 1998], and areal coverage data on crop types [*FAO*, 1998]. See color version of this figure at back of this issue.

biology and atmospheric dynamics and so that it could be used as a predictive tool. Finally, we wanted a model that would function on local to global spatial scales and hourly to interannual timescales so that spatial and temporal scales of the simulations would be comparable to the spatial and temporal scales represented by data collected at both flux towers and flask stations.

[5] The intent of this paper is to (1) present the mechanics of a model and simulation of terrestrial carbon isotope discrimination, (2) present the results of a global simulation at 1° resolution that is driven by observed meteorology and satellite-derived vegetation characteristics, and (3) evaluate simulation results by comparing them to observations taken at different temporal and spatial scales. Specifically, we compare (1) the simulated relationship between $\delta^{13}C$ of assimilated carbon and mean daily vapor pressure deficit (vpd) to field data from *Bowling et al.* [2002]; (2) the simulated relationship between $\delta^{13}C$ of assimilated carbon and monthly precipitation to field data from *Ometto et al.* [2002]; (3) mean $\delta^{13}C$ ratios for four biomes (Broadleaf, Temperate Broadleaf, Temperate Conifer, and Boreal) to observed $\delta^{13}C$ of ecosystem respiration from those biomes [*Pataki et al.*, 2003]; and (4) zonal mean assimilation-weighted $\delta^{13}C$ ratios of terrestrial biomass for 20°N to 60°N to $\delta^{13}C$ ratios of CO_2 fluxes inferred for terrestrially dominated stations of the NOAA Globalview Flask Network in the same latitude band [*Miller et al.*, 2003].

2. Method

[6] SiB2 is a model of the terrestrial biosphere that calculates surface fluxes of sensible and latent heat, radiation, moisture, CO_2, and momentum for vegetated land points [*Sellers et al.*, 1986, 1996a; *Denning et al.*, 1996a; *Schaefer et al.*, 2002]. SiB2 functions at local, regional, and global spatial scales, and can be driven by observed meteorology or coupled to a global climate model. In the present simulation, SiB2 is driven by assimilated meteorology for 1983–1993 provided by the European Centre for Medium-Range Weather Forecasting (ECMWF) with a 1° spatial resolution and a 6-hour time step (Figure 1) (see *Schaefer et al.* [2002] for more results from this particular simulation). ECMWF provides (1) wind speed at 10 m height, (2) temperature at 2 m, (3) relative humidity at 2 m, (4) total incident solar radiation, and (5) precipitation [*Gibson et al.*, 1999]. Time-varying phenological properties such as leaf area index (LAI), the fraction of photosynthetically active radiation absorbed by the green canopy

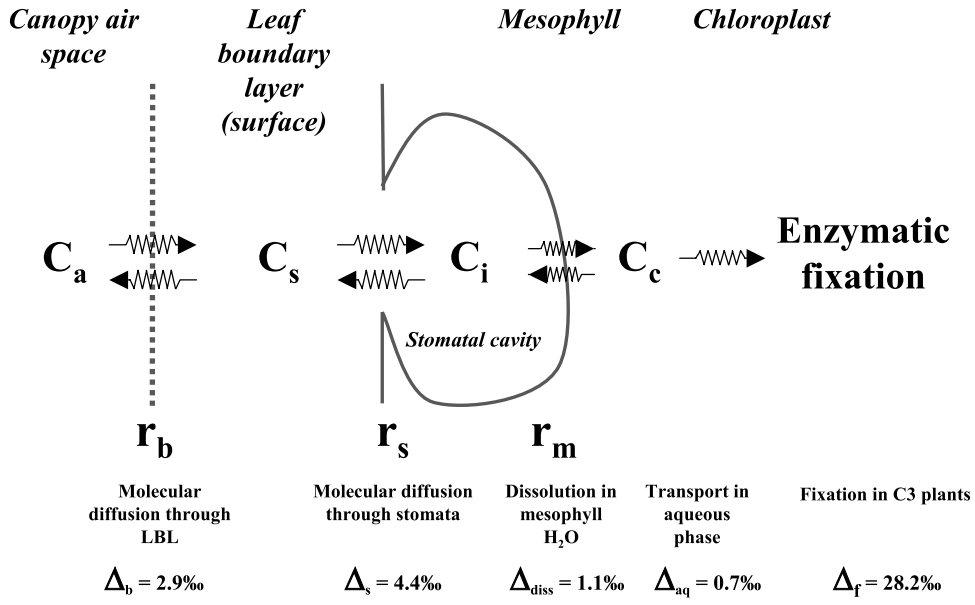

Figure 3. Schematic representation of carbon flow through C3 plants in CFRAX. C_a, C_s, C_i, and C_c are CO_2 partial pressures in the canopy, at the leaf surface, and in the stomatal cavity and chloroplast, respectively; r_b, r_s, and r_m are resistances to molecular diffusion of CO_2 across the leaf boundary layer, through the stomatal pore and from the stomatal cavity to the chloroplast, respectively; and Δ_b, Δ_s, Δ_{diss}, Δ_{aq}, and Δ_f are kinetic isotope effects accompanying molecular diffusion of CO_2 across the leaf boundary layer, through the stomatal pore, and from the stomatal cavity to the chloroplast (dissolution plus aqueous transport) and enzymatic fixation, respectively [*Craig*, 1953; *Mook et al.*, 1974; *Farquhar*, 1983; *O'Leary*, 1984].

(FPAR), and canopy greenness fraction are linearly interpolated each day from monthly maps of processed normalized difference vegetation index (NDVI) calculated from AVHRR red and near-infrared reflectance [*Los*, 1998; *Los et al.*, 2000]. Vegetation type is from *Defries and Townshend* [1994]. Other constant parameters, including canopy height and soil properties, are from look-up tables [*Zobler*, 1986; *Sellers et al.*, 1996b]. The distribution of C3 and C4 plants (Figure 2) [*Still et al.*, 2003] is determined using remote sensing products [*Defries and Townshend*, 1994; *DeFries et al.*, 1998, 1999a, 1999b, 2000], physiological modeling [*Collatz et al.*, 1998], crop fraction maps [*Ramankutty and Foley*, 1998], and areal coverage data on crop types [*Food and Agriculture Organization* (*FAO*), 1998]. Spatial resolution in the simulation is $1^\circ \times 1^\circ$. Recent improvements to SiB2 include the introduction of a six-layer soil temperature submodel based on the work of *Bonan* [1996, 1998] and a revised surface energy budget that includes prognostic temperature and moisture of the canopy air space reservoir [*Baker et al.*, 2003]. The calculations are implicit and allow for canopy storage, i.e., memory. Model results have been evaluated at local scales [*Baker et al.*, 2003], regional scales [*Denning et al.*, 2003; *Nicholls et al.*, 2004] and global scales [*Denning et al.*, 1996b].

[7] Another major change to SiB2 is the introduction of a scheme for calculating carbon isotope ratios of terrestrial CO_2 fluxes. Discrimination against ^{13}C during C3 photosynthesis is the result of a multistage process (Figure 3) involving relatively small isotope effects during transport of CO_2 from the canopy to the chloroplast and a large isotope effect associated with fixation by ribulose bisphosphate carboxylase/oxygenase (rubisco). Similar to equation (A6) in the Appendix of *Farquhar and Richards* [1984], we model this with three transport steps: (1) molecular diffusion across a laminar boundary layer at the leaf surface, (2) molecular diffusion through a stomatal pore into the stomatal cavity, and (3) dissolution into mesophyll water and aqueous transport to the chloroplast. This is followed by fixation with rubisco or other enzymes. Unlike *Farquhar and Richards* [1984], we do not include isotope effects associated with either dark respiration or photorespiration. This is because these effects are poorly characterized and probably quite small [*Farquhar et al.*, 1989; *O'Leary*, 1993; *Brugnoli and Farquhar*, 2000]. During photosynthesis, a CO_2 concentration gradient from the atmosphere to the chloroplast produces a flux into the plant. At each step, there is a slightly different CO_2 concentration which we designate as follows: C_a is CO_2 in the canopy air, C_s is CO_2 in the leaf boundary layer, C_i is CO_2 in the stomatal cavity, and C_c is CO_2 at the chloroplast. A resistance modulates transport from one step to the next: r_b for transport from the canopy air into the leaf boundary layer, r_s for transport through the stomatal pore, and r_c for transport to the chloroplast. These steps are also associated with isotope effects discriminating against ^{13}C: Δ_b, Δ_s, Δ_{diss}, and Δ_{aq}, respectively. Finally, there is an isotope effect during enzymatic fixation with rubisco, Δ_f. The Δ values that we use are Δ_b = 2.9‰, Δ_s = 4.4‰, Δ_{diss} = 1.1‰, Δ_{aq} = 0.7‰,

and Δ_f = 28.2‰, where Δ is defined as follows. For the reaction A $\rightarrow$ B,

$$\Delta_{AB} = 1000 \cdot (\alpha_{AB} - 1) \quad (1)$$

$$\alpha_{AB} = R_A/R_B = (\delta_A + 1000)/(\delta_B + 1000), \quad (2)$$

where $R_A = [^{13}C/^{12}C]_A$ $\delta_A = (R_A/R_{\mathrm{PDB}} - 1) \times 1000$ and R_{PDB}, the $^{13}C/^{12}C$ ratio of Pee Dee Belemnite, is equal to 0.0112372 [*Craig*, 1957]. Units for δ and Δ are per mil (‰). $\Delta = (\delta_A - \delta_B)/(\delta_B/1000 + 1) \approx (\delta_A - \delta_B)$. Δ_s and Δ_b are from theoretical calculations of molecular diffusion of CO_2 through air and across a laminar boundary layer [*Craig*, 1953; *Farquhar*, 1983]. Δ_{diss} and Δ_{aq} are from laboratory measurements [*Mook et al.*, 1974; *O'Leary*, 1984]. At the chloroplast, CO_2 can react with rubisco or other enzymes. The fraction reacting with other enzymes is not well known. *Raven and Farquhar* [1990] have suggested that the upper limit is about 10%. In our simulation, Δ_{f} is calculated by assuming that 92.5% of the assimilated CO_2 reacts with rubisco with an isotope effect of 30.0‰ [*Brugnoli and Farquhar*, 2000], while the remaining reacts with phosphoenyl pyruvate carboxylase (PEPC), with an isotope effect of 5.7‰ [*Farquhar*, 1983], giving a net isotope effect (Δ_f) of 28.2‰. Total isotope fractionation during C3 photosynthesis (ΔPS_{C3}) is given by sum of the concentration gradient-weighted isotope effects for each stage,

$$\Delta PS_{\mathrm{C_3}} = \Delta_b\left(\frac{C_a - C_s}{C_a}\right) + \Delta_s\left(\frac{C_s - C_i}{C_a}\right) + \left(\Delta_{\mathrm{diss}} + \Delta_{\mathrm{aq}}\right)\left(\frac{C_i - C_c}{C_a}\right) + \left(\Delta_f\right)\frac{C_c}{C_a}. \quad (3)$$

[8] In the present simulation, C_a is held constant at 35 Pa, though it can also be allowed to fluctuate naturally in order to isolate the effects of a dynamic canopy air space on $\delta^{13}C$ of biospheric CO_2 fluxes. Net assimilation (A_n, where A_n is gross photosynthesis minus aboveground autotrophic respiration) is calculated using a combination of Farquhar kinetics [*Farquhar et al.*, 1980] as modified by *Collatz et al.* [1991, 1992], and the Ball-Berry equation (4) for stomatal conductance (g_s, where $g_s = 1/r_s$) [*Ball*, 1988] [see *Sellers et al.*, 1996c, Appendix C].

$$g_s = m\frac{(A_n h_s)}{C_s} \times p + b, \quad (4)$$

where h_s is relative humidity at the leaf surface and is related to relative humidity of the canopy air through r_b and the transpiration rate, which is a function of wind speed and leaf geometry. Internal CO_2 concentrations (C_s, C_i, and C_c) are determined in an iterative loop that solves for internally consistent rates of A_n and C_c.

$$C_s = C_a - r_b A_n \times p, \quad (5)$$

$$C_i = C_s - r_s A_n \times p, \quad (6)$$

$$C_c = C_i - r_m A_n \times p. \quad (7)$$

Mesophyll conductance (g_m, where $g_m = 1/r_m$) is calculated using the following equation:

$$g_m = 4000 \times \mathrm{vmax0} \times \Pi \times \mathrm{RSTFAC}, \quad (8)$$

where vmax0 is the maximum rate of photosynthesis of sunlit leaves at the top of the canopy and is derived from the literature. Π is an integrating factor that expresses photosynthetic rate of the entire canopy as a function of the top leaf rate and the ability of the canopy to use photosynthetically active radiation (PAR). Π is strongly influenced by changes in NDVI. RSTFAC is a soil water stress factor [*Sellers et al.*, 1996a] (see also *Evans and Loretto* [2000] and references therein for a discussion of the effects of soil water stress on mesophyll conductance). Four thousand is a constant used to adjust mesophyll conductance to achieve a drop in CO_2 pressure between C_i and C_c of about 8 Pa at high rates of photosynthesis [*Evans and Loretto*, 2000].

[9] C4 photosynthesis also discriminates against ^{13}C, but to a much lesser extent. In C4 plants, CO_2 is "captured" in the stomatal cavity and transported to the site of enzymatic fixation with PEPC. Since nearly all of the CO_2 that reaches the site of fixation in C4 plants is assimilated, the kinetic isotope effects that are expressed are largely those involved in transport. Consequently, in this model we assume that carbon isotopic discrimination in C4 plants is constant and equal to the isotope effect associated with diffusion through the stomatal pore, i.e., ΔPS_{C4} = 4.4‰.

[10] There have been several previous studies modeling global terrestrial discrimination [*Lloyd and Farquhar*, 1994; *Fung et al.*, 1997; *Kaplan et al.*, 2002]. These studies differ from ours in the following ways (Table 1). Lloyd and Farquhar calculate monthly net assimilation as a simple function of climatologic monthly mean 0.5° $\times$ 0.5° temperature and precipitation [*Friedlingstein et al.*, 1992; *Leemans and Cramer*, 1991] and monthly 2.5° $\times$ 2.5° wet and dry bulb temperatures from ECMWF. Landcover is from *Wilson and Henderson-Sellers* [1985]. Stomatal CO_2 concentrations are calculated using an analytic model of optimal stomatal behavior with respect to water use efficiency. Chloroplast CO_2 concentrations are based on observed relationships between canopy CO_2, stomatal CO_2, and chloroplast CO_2. C3 discrimination is calculated using an equation similar to (3), although they include effects of autotrophic respiration and photorespiration and neglect the effect of transport across the leaf boundary layer. The effect of both of these differences on net discrimination is small. C3/C4 distributions in the work of Lloyd and Farquhar are based on a combination of physiological modeling and landcover maps from *Wilson and Henderson-Sellers* [1985]. C4 plants account for 21% of global GPP. C4 discrimination is a function of internal CO_2 concentrations and the leakiness of the bundle sheath cells. Net global C4 discrimination in the work of Lloyd and Farquhar is 3.6‰. Total discrimination (C3 and C4) in the work of Lloyd and Farquhar is 14.8‰; C3 discrimination is 17.8‰.

Table 1. Comparison of the Most Important Features and Results From Three Previous Studies of Global Carbon Isotope Fractionation of the Terrestrial Biosphere to Those of the Present Study[a]

Study	Net Assimilation	Internal CO_2 Concentrations	C3 Discrimination Calculations	C3/C4 Ratios	C4 Discrimination, ‰	C3 Discrimination, ‰	Net Discrimination, ‰
Lloyd and Farquhar [1994]	calculated using climatologic monthly mean 0.5° × 0.5° temperature and precipitation and 2.5° × 2.5° wet and dry bulb temperatures from ECMWF	internal CO_2 calculated using observed relationships between canopy, stomatal, and chloroplast CO_2 concentrations	calculated similarly to equation (3) except that isotope effects of photorespiration and autotrophic respiration are included and leaf boundary layer effects are not	on the basis of physiological modeling and landcover maps; C4 plants account for 21% of GPP	variable; averages 3.6‰; calculated based on internal CO_2 concentrations and leakiness of bundle sheath cells	17.8‰	14.8‰
Fung et al. [1997]	monthly mean 4° × 5° net assimilation from SiB2 coupled to global climate model	uses monthly assimilation-weighted Ci/Ca ratios calculated in SiB2, which simultaneously solves for Ci, stomatal conductance and net assimilation	two-step model that includes transport into stomatal cavity followed by fixation with rubisco	assumes that savannas are 75% C4 and land areas with shrubs are 50% C4; C4 plants account for 27% of GPP	fixed at 4.4‰	20.0‰	15.7‰
Kaplan et al. [2002]	net assimilation modeled in BIOME4, driven by 0.5° × 0.5° climatology (Climate 2.2)	calculated water-limited Ci/Ca ratios in a process-based model of canopy conductance	C3 discrimination is calculated in a similar fashion to Lloyd and Farquhar	vegetation, including C3/C4 ratios, is from a dynamic vegetation model with an agricultural mask; C4 plants account for 15% of GPP	calculated similarly to Lloyd and Farquhar	20.0 ± 1.0‰	18.1‰ with the agricultural mask or 18.6‰ without it
This study	we determine net assimilation rates each 10 min using SiB2.5, which is driven by 6-hourly assimilated meteorology from ECMWF; vegetation parameters are constrained by satellite observations, i.e., FASIR-NDVI	each time step we simultaneously solve for Cc, stomatal conductance, and net assimilation; other internal CO_2 concentrations are functions of net assimilation and internal resistances	C3 discrimination is calculated using a four-step model that includes transport across the leaf boundary layer, through the stomatal pore, aqueous phase transport, and fixation with rubisco	C3/C4 ratios are calculated using physiological modeling, satellite observations and agricultural maps; C4 plants account for 24% of GPP	fixed at 4.4‰	19.2‰	15.9‰

[a]Please see text for detailed references.

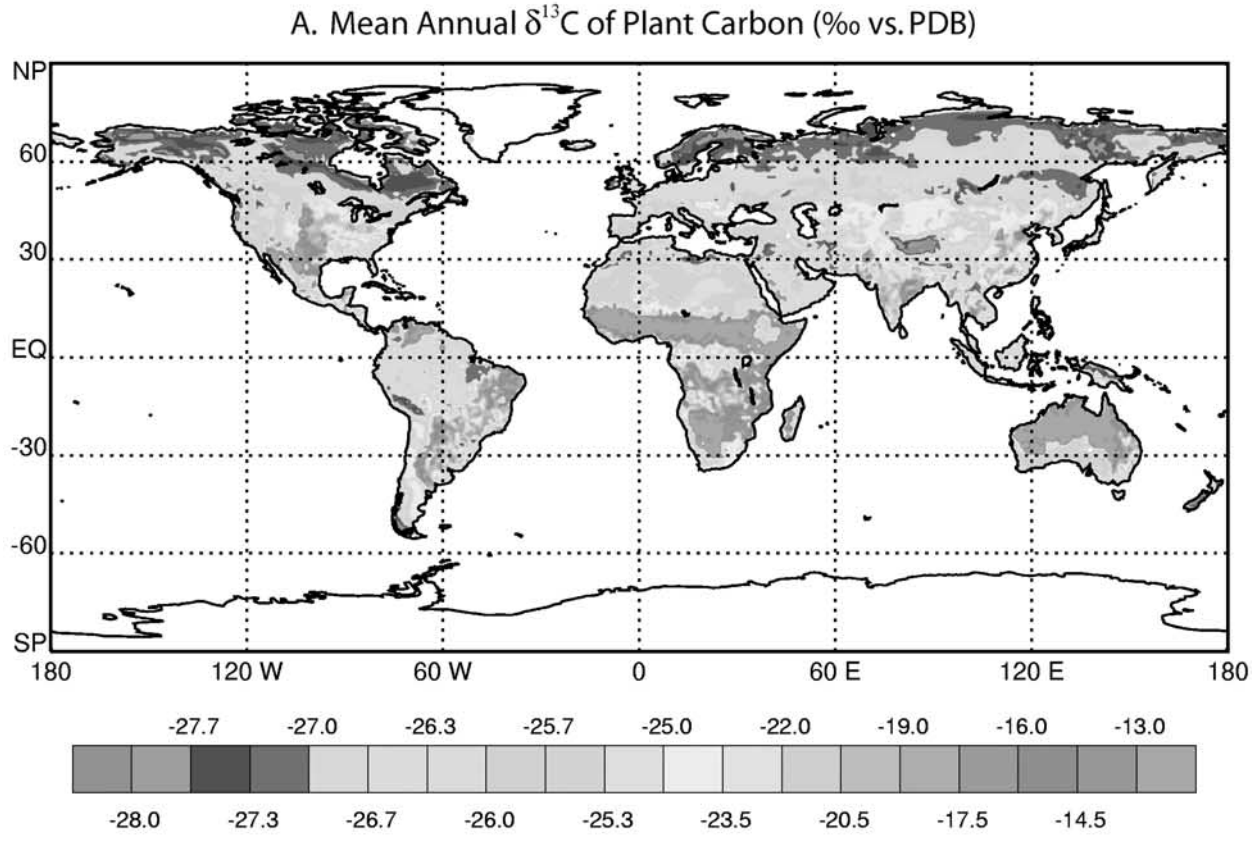
A. Mean Annual δ13C of Plant Carbon (‰ vs. PDB)
NP
60
30
EQ
-30
-60
SP
180
120 W
60 W
0
60 E
120 E
180
-27.7
-27.0
-26.3
-25.7
-25.0
-22.0
-19.0
-16.0
-13.0
-28.0
-27.3
-26.7
-26.0
-25.3
-23.5
-20.5
-17.5
-14.5

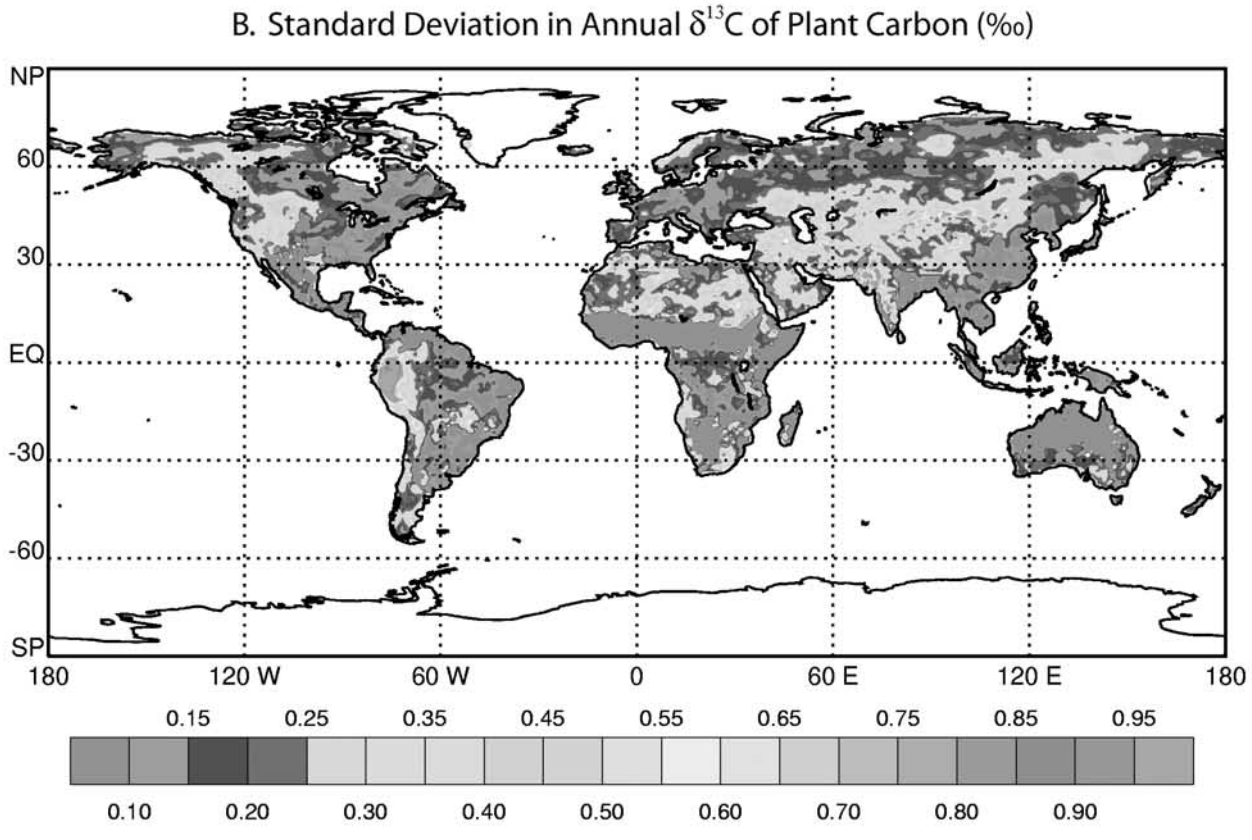
B. Standard Deviation in Annual δ13C of Plant Carbon (‰)
NP
60
30
EQ
-30
-60
SP
180
120 W
60 W
0
60 E
120 E
180
0.15
0.25
0.35
0.45
0.55
0.65
0.75
0.85
0.95
0.10
0.20
0.30
0.40
0.50
0.60
0.70
0.80
0.90

Figure 4

[11] *Fung et al.* [1997] calculate net assimilation at a $4° \times 5°$ resolution using monthly mean output from an older version of SiB2 coupled to a global climate model [*Sellers et al.*, 1996a, 1996b; *Randall et al.*, 1996]. Fung et al. calculate net assimilation-weighted C_i/C_a ratios by simultaneously solving for C_i, stomatal conductance, and net assimilation. Discrimination is based on a two-step model of photosynthesis that includes only transport of CO_2 into the leaf, followed by enzymatic fixation. Fung et al. assume that savannas are 75% C4 and land areas covered by shrubs and groundcover are 50% C4. C4 plants make up 27% of GPP. C4 discrimination is fixed at 4.4‰. Total discrimination in the work of Fung et al. is 15.7‰; C3 discrimination is 20.0‰.

[12] *Kaplan et al.* [2002] calculate net assimilation using a model of the terrestrial biosphere (BIOME4) driven by $0.5° \times 0.5°$ gridded climatology (Climate 2.2), which is an updated version of work by *Leemans and Cramer* [1991]. Vegetation, including C3/C4 distributions, is determined in a dynamic vegetation model with an agricultural mask. Kaplan et al. calculate water-limited C_i/C_a ratios in a process-based model of canopy conductance. The discrimination model is similar to that of Lloyd and Farquhar. C4 plant distributions in BIOME4 are determined in a dynamic vegetation model with an agricultural mask. C4 plants constitute only about 15% of global GPP, significantly less than suggested by the models here (J. O. Kaplan, personal communication, 2004), which range from 21% to 27% or the 18% estimated by *Ehleringer et al.* [1997]. C4 discrimination in the work of Kaplan et al. is determined in a manner similar to that of Lloyd and Farquhar. Discrimination for C4 plants is not given. Total discrimination in the work of Kaplan et al. is 18.6‰ or 18.1‰ with the agricultural mask; C3 discrimination is 20.0 ± 1.0‰. The higher total discrimination in the work of Kaplan et al. relative to the other models, as well as observations [*Bakwin et al.*, 1998; *Miller et al.*, 2003], is probably due largely to differences in global C3/C4 distributions.

[13] Our simulation calculates net assimilation each 10-min time step using an updated version of SiB2 coupled to assimilated 6-hourly $1° \times 1°$ weather from ECMWF for 1983 through 1993. We calculate internal CO_2 concentrations each time step in SiB2 as described earlier. One difference between our simulation and that of *Fung et al.* [1997] is that we calculate net assimilation solving for C_c instead of C_i. Discrimination is determined using equation (3). As Fung et al. point out, all other things being equal, neglecting isotope effects during transport of CO_2 from the stomatal cavity to the chloroplast can reduce total C3 discrimination by about 2–3‰. However, since we calculate net assimilation using C_c instead of C_i, net assimilation rates are lower and consequently the change in discrimination is much less than 2–3‰. We use C4 maps based on physiological modeling, satellite observations, and agricultural maps [*Still et al.*, 2003]. C4 plants constitute 25% of GPP. C4 discrimination is fixed at 4.4‰. Total discrimination in our study is 15.9‰; C3 discrimination is 19.2‰. A final feature of our discrimination module is that it can be coupled to a prognostic canopy air space and can thus be used to examine systematic variations between discrimination and transport on the time step of the simulation including recycling of respired CO_2 and Rayleigh-type distillation of canopy CO_2 during daytime photosynthesis.

[14] The $\delta^{13}C$ values reported here are weighted by assimilation. ^{12}C and ^{13}C fluxes are calculated separately for C3 and C4 plants and then summed to get grid values for each time step. At the end of the year, we divide by total net assimilation to retrieve the $\delta^{13}C$ of plant carbon assimilated within that grid cell during the preceding year. At the end of the 11-year run, we calculate mean and standard deviation of annual assimilation weighted $\delta^{13}C$ ratios for each $1° \times 1°$ grid cell. Since we want to focus here on the response of the terrestrial discrimination to climate variations, we hold the concentration and carbon isotope ratio of canopy CO_2 constant. This necessarily neglects the influence of variations in $\delta^{13}C$ of canopy CO_2 on $\delta^{13}C$ of assimilated carbon due to (1) recycling of respired CO_2, (2) enrichment of canopy CO_2 in ^{13}C due to preferential of removal of ^{12}C during photosynthesis, (3) turbulent mixing with the atmospheric boundary layer, and (4) seasonal variations in $\delta^{13}C$ of atmospheric CO_2. A subsequent analysis will evaluate the influence of a dynamic canopy on $\delta^{13}C$ of terrestrial fluxes.

3. Results and Discussion

3.1. Spatial Variations in $\delta^{13}C$ of Plant Carbon

[15] Spatial variations in $\delta^{13}C$ of plant carbon are complex and reflect climate, water availability, biome type and C3/C4 distributions (Figure 4a). In general, the lightest $\delta^{13}C$ values for are found at high northern latitudes and reflect both the absence of C4 plants and increased discrimination in C3 plants due to zonal variations in the modeled C_c/C_a ratio. The starkest contrasts globally are those produced by variations in C3/C4 distributions. There is a zonal trend to this distribution and its influence on $\delta^{13}C$; that is, the heaviest $\delta^{13}C$ values are found approximately 10° to 20° north and south of the equator, mirroring the distribution of C4 grasslands.

Figure 4. (a) Mean annual assimilation-weighted $\delta^{13}C$ of terrestrial plant carbon from an 11-year simulation (1983–1993) and (b) standard deviation in annual $\delta^{13}C$ values. During each time step, net assimilation is multiplied by the $\delta^{13}C$ of assimilated plant carbon. At the end of the year, the sum of net assimilation times $\delta^{13}C$ is divided by total annual net assimilation to give the $\delta^{13}C$ value of carbon assimilated in each grid cell during that calendar year. The mean is the average of the 11 annual values. The standard deviation is also for those 11 values. Please note the higher resolution used in reporting more negative mean values (Figure 4a). This is done in order to highlight spatial variations in C3 discrimination. There is tremendous spatial variability in $\delta^{13}C$ values of terrestrial carbon. The sharpest spatial contrasts are the result of differences in C3/C4 ratios. Variation in $\delta^{13}C$ values of C3 plants is largely driven by differences in relative humidity during the growing season. Larger than average standard deviations are found in areas where ECMWF predicts significant variations in annual precipitation. See color version of this figure at back of this issue.

Table 2. Simulated $\delta^{13}C$ of Total Plant Carbon and $\delta^{13}C$ of C3 Plant Carbon[a]

Biome	n	$\delta^{13}C_{Tot}$, ‰	$\delta^{13}C_{C3}$, ‰
Broadleaf Evergreen	1098	−25.0 ± 2.8	−26.6 ± 0.34
Broadleaf Deciduous	320	−21.9 ± 4.9	−25.9 ± 1.2
Broadleaf and Needleleaf	769	−25.4 ± 1.9	−26.3 ± 0.42
Needleleaf	2018	−27.1 ± 0.6	−27.1 ± 0.41
Needleleaf Deciduous	952	−26.6 ± 0.4	−26.6 ± 0.38
Broadleaf With Groundcover	1457	−18.3 ± 4.6	−26.5 ± 0.89
Groundcover (maize optical)	779	−15.4 ± 4.4	−25.8 ± 1.6
Broadleaf Shrubs and Bare Soil	1035	−21.3 ± 6.0	−25.4 ± 1.1
Tundra and Dwarf Trees	1528	−27.0 ± 0.5	−26.9 ± 0.50
Low-Latitude Deserts	1602	−25.7 ± 2.2	−26.0 ± 0.87
Broadleaf Deciduous Over Wheat	3079	−24.3 ± 3.3	−25.8 ± 0.73

[a]Values are means and standard deviations for all grid cells within the biome from the map of 11-year mean values. The $\delta^{13}C$ values of plant carbon are based on a $\delta^{13}C$ value for atmospheric CO_2 of −7.9‰ versus PDB.

However, there are also important longitudinal patterns in $\delta^{13}C$ values that are produced not only by C3/C4 distributions, but also by variations in climate and biome type. Examples of this include the influence of high C4 ratios in the North American Plains and African Sahel on $\delta^{13}C$ of terrestrial biomass of the Western and Eastern Hemispheres. Table 2 presents $\delta^{13}C$ ratios of all plants ($\delta^{13}C_{Tot}$) and C3 plants only ($\delta^{13}C_{C3}$) broken down by biome.

[16] The standard deviations in annual $\delta^{13}C$ values for individual grid cells for the 11 years are generally less than 0.3‰ (Figure 4b). The largest standard deviations are generally found in areas where ECMWF predicts large variations in annual precipitation and occasional drought. The most prominent example is the western and southern edges of the Amazon basin, which in ECMWF reanalysis experienced significantly drier conditions in 1983–1986, relative to the rest of the 11-year simulation.

3.2. Evaluation of Model Results

3.2.1. C3 Discrimination and Vapor Pressure Deficit

[17] Laboratory and field studies show that discrimination in C3 plants is largely controlled by the influence of vapor pressure deficit (vpd) on stomatal conductance and C_c/C_a ratios [*Farquhar and Richards*, 1984; *Farquhar et al.*, 1982, 1989; *Berry*, 1988; *Condon et al.*, 1993; *Hall et al.*, 1993]. Since vpd of canopy air changes over the course of the day and from one day to the next, carbon isotope discrimination should change just as quickly. Until recently, however, it has been difficult to quantify changes in discrimination in natural ecosystems on these short timescales.

[18] Nighttime Keeling plot intercepts record $\delta^{13}C$ of respired CO_2 fluxes ($\delta^{13}C_R$) from aboveground (bole, stem, leaf, and heterotrophic) and belowground (root and decomposing soil organic matter) sources [*Keeling*, 1958]. *Högberg et al.* [2001] have shown that tree girdling reduced soil respiration by up to 37% after only 5 days, indicating that roots are responsible for approximately 40% of the total soil CO_2 flux. Using the fact that $\delta^{13}C$ of root respiration reflects the carbon isotope ratio of recent photosynthate [*Andrews et al.*, 1999; *Lin et al.*, 1999], *Ekblad and Högberg* [2001] and *Bowling et al.* [2002] then demonstrated that variations in $\delta^{13}C$ of ecosystem respiration are strongly correlated with changes in relative humidity and/or vapor pressure deficit that have occurred within the previous 2 to 10 days. Consequently, changes in nighttime Keeling plot intercepts reflect humidity-induced changes in discrimination through the release of recently fixed carbon during autotrophic respiration.

[19] In order to evaluate the ability of our model to accurately represent the relationship between C3 discrimination and relative humidity, we compare simulated mean daily vapor pressure deficits and assimilation-weighted $\delta^{13}C$ values for C3 plants to the observed relationships (Figure 5). We have chosen sites similar to those presented by *Ekblad and Högberg* [2001] and *Bowling et al.* [2002], as well as others spanning a range of vapor pressure deficits and biomes. In general, the model successfully captures the relationship between vpd and $\delta^{13}C$ and is bracketed by the observations. However, there are differences between model results and observation that are worth noting. The $\delta^{13}C$ values in the simulation are similar to those observed by Ekblad and Högberg, but slightly less negative than those of Bowling et al. There are a couple of reasons that it is difficult to assess the importance of these absolute differences in $\delta^{13}C$ values. First, both sets of observations include undetermined offsets due to the fact that the $\delta^{13}C$ of decomposing soil organic matter (SOM) is unknown. In general, CO_2 from decomposing SOM is thought to be enriched in ^{13}C relative to recently fixed photosynthate as a consequence of a terrestrial "Suess Effect" [e.g., *Ciais et al.*, 1999]. On the basis of flux-weighted ages of decomposing SOM [*Fung et al.*, 1997] and a long-term record of $\delta^{13}C$ of atmospheric CO_2 [*Francey et al.*, 1999], we might expect $\delta^{13}C$ of SOM in northern Sweden to be enriched relative to recent photosynthate by about 0.7‰, whereas the sites of Bowling et al. would be slightly less enriched and more variable (0.2‰ to 0.7‰). However, these are only rough estimates, and more would have to be known about the age and turnover rate of the SOM at specific sites to be more precise. If decomposing soil organic matter produced 60% of the soil CO_2 flux, a 0.7‰ offset would mean that $\delta^{13}C$ of recently fixed carbon was approximately 0.4‰ more negative than observations indicate. Another problem with comparing the two studies is that they use slightly different methodologies. The differences include: (1) different methods were used for collecting and analyzing gas samples, (2) Ekblad and Högberg looked at a single site, whereas Bowling et al. used four sites, (3) Ekblad and Högberg used a 2- to 3-day lag time, whereas Bowling et al. used lag times ranging from 5 to 10 days, and (4) Ekblad and Högberg took climate data from a weather station at the site, whereas Bowling et al. had to infer climatic conditions from stations located farther afield. Finally, Ekblad and Högberg fit the data to a linear equation, while Bowling et al. were more successful with a logarithmic fit. Nevertheless, the simulated results are consistent with both studies, and both the model and observations show that stomatal response to changes in vapor pressure

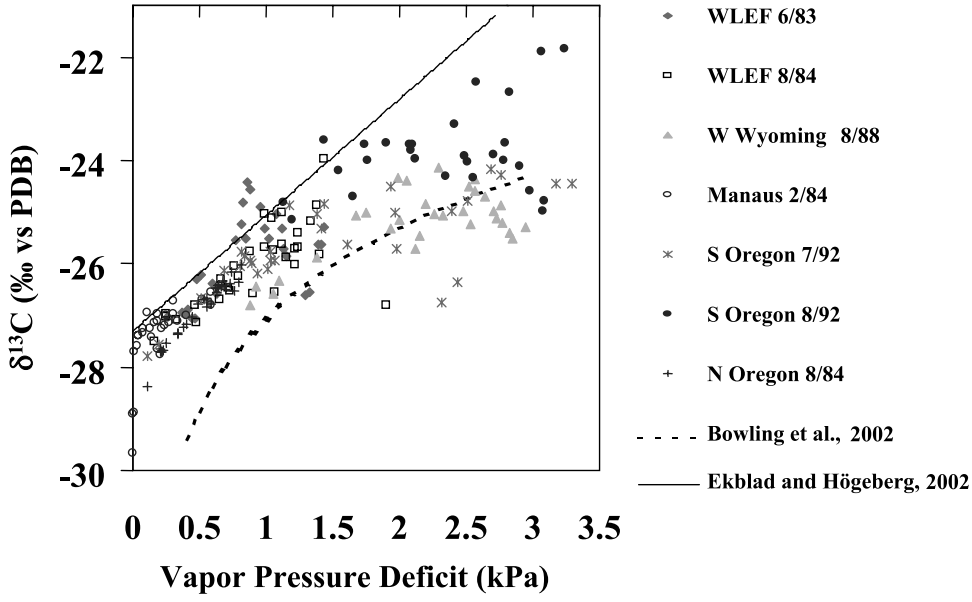

Figure 5. Relationship between vapor pressure deficit (vpd), i.e., the difference between saturated water vapor pressure and vapor pressure of the canopy air, and $\delta^{13}C$ of ecosystem respiration ($\delta^{13}C_R$) by C3 plants. The two lines are from observations. The data points are from the simulation. The solid line is the proposed linear fit to measurements from a mixed coniferous boreal forest in northern Sweden ($y = 0.2242x - 27.3$; $r2 = 0.94$, $n = 5$) [see *Ekblad and Högberg*, 2001, Figure 3]. Meteorologic data were collected at a weather station 200 m from the site. The vpds are calculated from the 2-day mean for maximum air temperature and the 2-day mean relative humidity at the maximum air temperature. The dotted line is a simple logarithmic fit to data proposed by *Bowling et al.* [2002] ($y = 2.54\text{Ln}x - 27.8$; $r^2 = 0.79$, $n = 22$; see Figure 7). The curve is constructed from 22 points from four sites in Oregon. Bowling et al. calculated vpd using either on-site instrumentation or data from Oregon Climate service stations as near to the site as possible. The $\delta^{13}C_R$ values are constructed from 2-day averages of Keeling plot intercepts using geometric mean regressions of nocturnal data. Since there is likely to be a delay between the time the carbon is photosynthetically fixed and the time that it is respired, in the observations a time lag was selected by looking for the best statistical fit between $\delta^{13}C_R$ and 2-day mean vpd over varying time periods. Although Ekblad and Högberg used a 3- to 4-day time lag for the relationship between $\delta^{13}C_R$ and relative humidity, a 2- to 3-day lag was best for fitting $\delta^{13}C_R$ and vpd; Bowling et al. used time lags ranging from 5 to 10 days, depending on the site. Data points are from the simulation and are mean daily vpd for daylight hours only and assimilation-weighted $\delta^{13}C$ values. The red solid circles, blue stars, and green crosses are from grid boxes in Oregon which are similar to the locations in the Bowling et al. study. Other data points are from sites and months intended to represent a range of conditions from very wet to very dry. The locations are as follows: WLEF (45.5°N, 90.5°W); W Wyoming (41.5°N, 109.5°W); Manaus (2.5°S, 55.5°W); N Oregon (48.5°N, 124.5°W); and S Oregon (43.5°N, 123.5°W). In the simulation, $\delta^{13}C$ of canopy CO_2 is held constant at −7.9‰.

deficit in the canopy air is a dominant control on discrimination on diurnal timescales.

3.2.2. C3 Discrimination and Monthly Precipitation

[20] *Ometto et al.* [2002] examine the relationship between C3 discrimination and monthly precipitation in tropical forest sites of the Amazon basin. In data collected near Santarém, Brazil, there is an inverse relationship between $\delta^{13}C$ of ecosystem respiration ($\delta^{13}C_R$) and monthly precipitation that persists at rain rates up to 300 mm/month. At much higher rates of precipitation, i.e., greater than 400 mm/month, the relationship appears to reverse. They argue that at the lower rain rates, changes in $\delta^{13}C_R$ are controlled by stomatal-induced variations in C3 discrimination caused by a combination of soil water stress and relative humidity. It is unclear why discrimination decreases at precipitation rates greater than 400 mm/month. Ometto et al. also collected data from a second tropical forest site near Manaus, Brazil. At Manaus, the relationship between $\delta^{13}C_R$ and monthly precipitation is less clear, even though the site is similar in many respects to that of Santarém.

[21] We examined the relationship between monthly precipitation and C3 discrimination in the simulation for the grid cell containing Santarém, Brazil, as well as a temperate forest grid cell containing the WLEF tall tower site in Wisconsin (Figure 6). In the simulation, C3 discrimination increases with increasing monthly precipitation. The relationship is slightly nonlinear, with a steeper slope at very low rates of precipitation. In other words, changes in

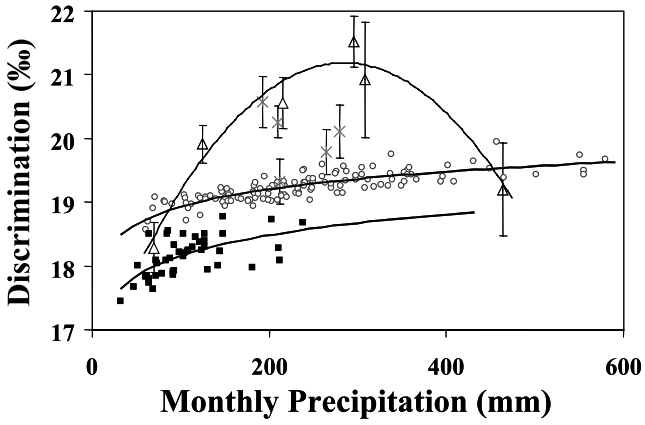

Figure 6. Relationship between monthly precipitation and C3 discrimination. Discrimination has been converted from del values using the formula: Discrimination = $(\delta^{13}C_{air} - \delta^{13}C_R)/(1 - \delta^{13}C_{air}/1000)$; where $\delta^{13}C_{air} = -7.9‰$ and $\delta^{13}C_R$ is the carbon isotope ratio of ecosystem respiration. Triangles and asterisks are from measurements in primary evergreen tropical forests: triangles (Santarém, Brazil), asterisks (Manaus, Brazil) [see *Ometto et al.*, 2002, Figure 7]. The error bars represent the standard error of the isotope measurement. The curve is a second-order polynomial fit to the data from Santarém. The open circles are simulated discrimination for the grid box containing Santarém. Simulated data from Manaus are nearly identical. The solid squares are simulated discrimination for summer months for the grid box containing WLEF tower in Wisconsin. The lines through the simulated data are logarithmic fits to the data.

precipitation rates have a greater impact on carbon isotope discrimination under very dry conditions than they do when the environment is already wet. Discrimination at WLEF is about 1‰ less than that predicted for Santarém, largely because of the greater relative humidity of the tropical forested site. Model results agree with the observations to the extent that we predict a positive correlation between monthly precipitation and discrimination; however, there are several important differences between the model and observations. First, observed $\delta^{13}C_R$ for both Santarém and Manaus is depleted in ^{13}C by up to 2‰ relative to modeled discrimination. Second, the slope of the relationship in the observations at Santarém is about 3 times greater than the slope predicted for the grid cell containing Santarém. In the observations, $\delta^{13}C$ of ecosystem respiration decreases by approximately 3‰ for changes in precipitation from 50 to 300 mm/month; in the simulation, the change is closer to 1‰. Third, at Santarém, $\delta^{13}C$ of ecosystem respiration returns to heavier values at precipitation rates greater than 400 mm/month, whereas modeled discrimination continues to increase with increasing precipitation rates.

[22] Reasons for the enrichment in modeled values relative to observations at both Santarém and Manaus will be addressed later in the paper. With respect to the relationship between discrimination and monthly precipitation, we think that there may be several reasons for the differences between the model and observations at Santarém. First, while we have no reason to doubt the results of *Ometto et al.* [2002], the question must be asked: Is this site representative of tropical forest behavior in general? Data collected at Manaus do not refute the relationship observed at Santarém; however, neither do they confirm it. In part, this is because of the narrow range of monthly precipitation rates observed at Manaus; however, more data will have to be collected before we can say that the behavior at Santarém is characteristic of tropical forests in general. A second possibility is that there are important natural variations accompanying changes in monthly precipitation that are not captured in the model. The two most probable candidates are relative humidity and/or soil water. Since SiB2 seems to do a good job simulating the relationship between discrimination and vapor pressure deficit, the problem may be with the way that we model soil water stress. Throughout the 11 years of the simulation, there is no significant soil water stress on plant growth in the grid cell containing Santarém, even during the driest months. Unfortunately, we have no observations to directly compare to the simulation. Terrestrial ecosystem models sometimes predict decreases in photosynthetic rates during the tropical forest dry season due to drought stress; however, this decline in assimilation rates is not always supported by the observations [*Tian et al.*, 1998; *Saleska et al.*, 2003]. Finally, there is a similar

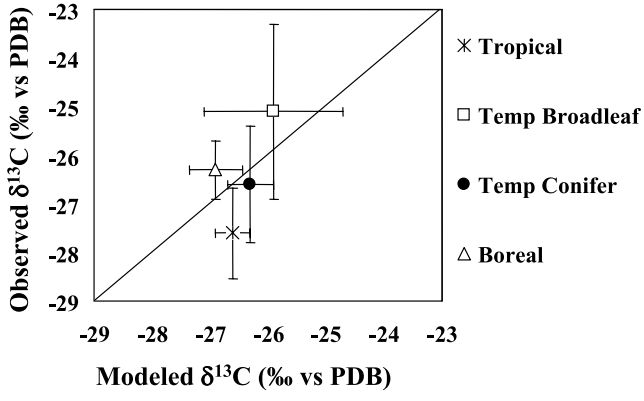

Figure 7. A comparison between simulated and observed $\delta^{13}C$ values of ecosystem respiration for four forest biome types. Observations are from the BASIN network [*Pataki et al.*, 2003]. Error bars are standard deviations. SiB2's broadleaf evergreen biome ($-26.6 \pm 0.3‰$, n = 1098) is compared to observations from tropical forests ($-27.6 \pm 0.94‰$, n = 5); broadleaf deciduous ($-25.9 \pm 1.2‰$, n = 318) is compared to temperate broadleaf ($-25.1 \pm 1.8‰$, n = 18); broadleaf and needleleaf ($-26.3 \pm 0.4‰$, n = 769) is compared to temperate conifer ($-26.6 \pm 1.2‰$, n = 13); and needleleaf ($-27.1 \pm 0.4‰$, n = 2017) and needleleaf deciduous ($-26.6 \pm 0.4‰$, n = 952) are combined ($26.9 \pm 0.5‰$, n = 2969) and compared to boreal ($-26.3 \pm 0.6‰$, n = 7). In general, simulated $\delta^{13}C$ values are close to observed values although there is slightly less variability in simulated values than in observations. In addition, simulated $\delta^{13}C$ values in the tropics are heavy relative to observed values.

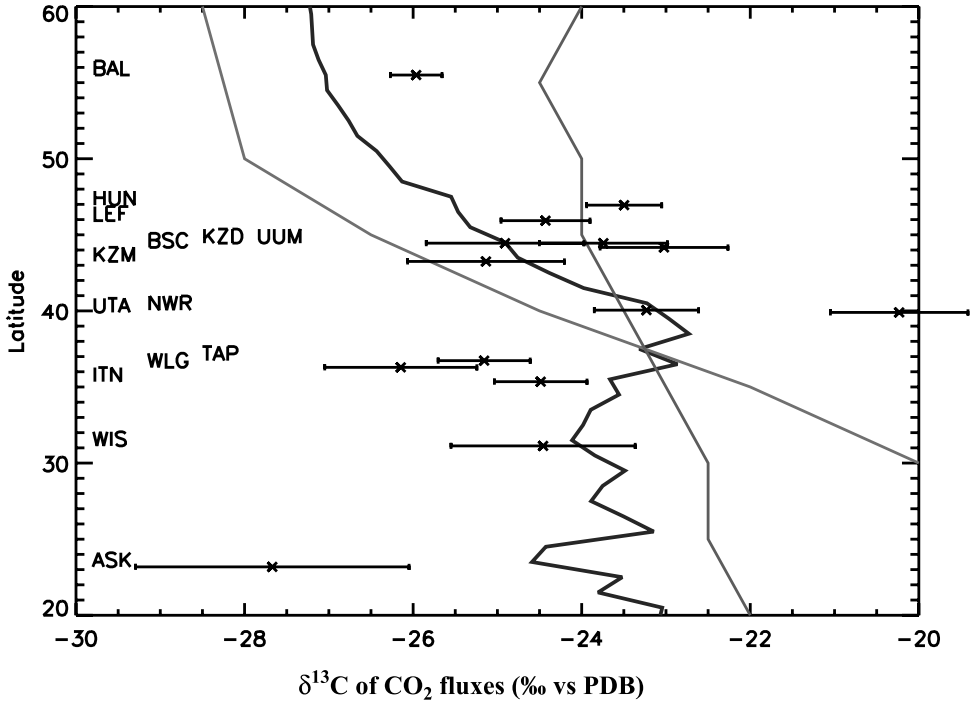

Figure 8. Zonal $\delta^{13}C$ ratios of terrestrial biosphere from *Miller et al.* [2003] (data points with error bars), *Lloyd and Farquhar* [1994] (red line), *Fung et al.* [1997] (green line), and this study (blue line). See color version of this figure at back of this issue.

pattern between observed mean carbon isotope composition of ecosystem respiration and mean annual precipitation; that is, discrimination increases with increasing precipitation up to a point, where it then returns to lower values at very high rain rates. In the simulation, annually integrated $\delta^{13}C$ values are generally more negative in wet climates, and they do not return to less negative values in extremely wet climates.

3.2.3. C3 Discrimination by Biome

[23] The number of measurements of $\delta^{13}C_R$ that have been collected is constantly increasing and can serve as an additional method for evaluating simulation results. Data for Figure 7 are taken from *Pataki et al.* [2003] and show mean $\delta^{13}C_R$ values and standard deviations for four different biomes: Broadleaf, Temperate Broadleaf, Temperate Conifer, and Boreal. We have plotted mean $\delta^{13}C_R$ values and standard deviations for comparable biomes from our simulation against the observed values. In general, simulated mean values are relatively close to the observed means, and the standard deviations encompass the range of observed values. However, there are a couple of important differences between the simulation and the observations. First, the mean model $\delta^{13}C_R$ for the tropical forests is 1‰ less negative than the mean of the observations. If simulated discrimination in the tropical forests is incorrect, it could be the result of a couple of factors. First, our estimate for maximum C3 discrimination (28.2‰) may be too small. This could be because the isotope effect that we use for CO_2 fixation with Rubisco (30‰) is not large enough, or because of our assumption that 7.5% of the carbon fixed by C3 plants occurs through reactions with PEPC is too great. Either one is a possibility. Measurements of isotope effects associated with rubisco are precise, but the values range from approximately 26‰ to 38‰ [*O'Leary*, 1981; *Brugnoli and Farquhar*, 2000]. With respect to the amount of CO_2 in C3 plants that reacts with PEPC, very little is known. A maximum of 10% has been suggested [*Raven and Farquhar*, 1990] and *Lloyd and Farquhar* [1994] assumed that it was 5%, so perhaps our estimate of 7.5% is too high. Changing from 7.5% to 5% reduces discrimination by about 0.6‰. Of course, while the change improves the match to observed $\delta^{13}C_R$ for tropical forests, it hurts the fit with Boreal and Temperate Broadleaf biomes. Another possibility is that there are biome-specific differences in this fraction of which we are unaware. A second reason why our $\delta^{13}C$ values for tropical forests are enriched in ^{13}C relative to observations could be due to the fact that we do not include the effects of recycling of isotopically depleted respired CO_2. In this study we hold $\delta^{13}C$ of canopy CO_2 constant at −7.9‰. Estimates of the amount of respired CO_2 that is recycled are as high as 30 to 40% [*Sternberg et al.*, 1997], although others have argued that it is actually quite negligible [*Lloyd et al.*, 1996, 1997]. In sensitivity tests in which we coupled the biosphere to a dynamic canopy, recycling was greatest in tropical forests, which is consistent with observations, and caused $\delta^{13}C$ of assimilated carbon to be depleted in ^{13}C by 1–4‰. Working against this effect, however, is an offset due to the terrestrial "Suess Effect." On the basis of flux-weighted ages of decomposing SOM [*Fung et al.*, 1997] and a long-term record of $\delta^{13}C$ of atmospheric CO_2 [*Francey et al.*, 1999], the terrestrial Suess Effect in tropics is estimated to be about +0.6‰, which would counter some of the effects of recycling. A second

and perhaps more important difference between the observations and the model is that there appears to be a wider range of values in the observations than in the model. Unfortunately, there are still so few observations that it is difficult to know how representative they are. Nonetheless, it is entirely possible that the wider range of values in the observations is due to heterogeneity within biomes that is not captured by the model.

3.2.4. Zonal Trends in $\delta^{13}C$ of Plant Carbon Compared to Atmospheric Data

[24] Results of the simulation can also be compared to atmospheric data. *Miller et al.* [2003] have analyzed high-frequency deviations from a seasonal spline fit to time series of CO_2 and $\delta^{13}C$ measurements from continental stations from the NOAA Globalview Flask Network in order to deduce the carbon isotopic ratios of growing season CO_2 fluxes in the Northern Hemisphere. They argue that these deviations from the seasonal signal are produced by fluxes to and from the local vegetation and are therefore a record of the isotopic ratio of that vegetation. Miller et al. have plotted the $\delta^{13}C$ values from these sites as a function of latitude, as well as zonal mean $\delta^{13}C$ values from *Fung et al.* [1997] and *Lloyd and Farquhar* [1994]. Their figure is recreated here with the addition of our zonal mean assimilation-weighted $\delta^{13}C$ values for the Northern Hemisphere growing season (Figure 8). While it is difficult to make a direct comparison, because the observations largely represent regional values of terrestrial discrimination, it appears that our zonal mean is an improvement over previous simulations in that it captures some of the flatness of the signal between 20°N and 40°N, as well as the rapid descent to more negative values north of 40°N. Furthermore, although we are still limited by a paucity of data, both observations and simulated results indicate that spatial distribution of $\delta^{13}C$ values of the terrestrial biosphere are more complex than previously thought.

4. Conclusion

[25] A multistage model of carbon isotope discrimination during photosynthesis and global maps of C3/C4 plant ratios coupled to an ecophysiological model of the terrestrial biosphere driven by observed meteorology and constrained by satellite-derived NDVI has been used to predict the carbon isotope ratios of terrestrial plant carbon. Simulated mean annual C3 discrimination for 1983–1993 is 19.2‰; total mean annual discrimination by the terrestrial biosphere (C3 and C4 plants) is 15.9‰.

[26] It is very difficult to constrain the details of the simulated results because we are still sorely lacking in observations. However, within these limitations we find the following. The modeled response to changes in vapor pressure deficit compares favorably to observations. Simulated monthly discrimination in tropical forests is less sensitive to changes in precipitation than is suggested by some observation. Mean model $\delta^{13}C$ ratios for Broadleaf, Temperate Broadleaf, Temperate Conifer, and Boreal biomes compare well with the few measurements available; however, there is more variability in observations than in the simulation, and modeled $\delta^{13}C$ values for tropical forests appear heavy relative to observations. Finally, simulated zonal $\delta^{13}C$ ratios in the Northern Hemisphere capture the complexity of the zonal $\delta^{13}C$ inferred from atmospheric measurements better than previous investigations.

[27] **Acknowledgments.** We would like to thank Inez Fung for helpful discussions. This work was funded by the NASA Earth Science Enterprise Interdisciplinary Science Program under contract NAS-31730 and the National Science Foundation under contract 00223464.

References

Andrews, J. A., K. G. Harrison, R. Matamala, and W. H. Schlesinger (1999), Separation of root respiration from total respiration using carbon-13 labeling during free air carbon dioxide enrichment (FACE), *Soil Sci. Soc. Am. J.*, *63*, 1429–1435.

Baker, I. T., A. S. Denning, N. Hanan, L. Prihodko, M. Uliasz, P.-L. Vidale, K. Davis, and P. Bakwin (2003), Simulated and observed fluxes of sensible and latent heat and CO_2 at the WLEF-TV tower using SiB2.5, *Global Change Biol.*, *9*, 1–16.

Bakwin, P. S., P. P. Tans, J. W. C. White, and R. J. Andres (1998), Determination of the isotopic ($^{13}C/^{12}C$) discrimination by terrestrial biology from a global network of observations, *Global Biogeochem. Cycles*, *12*, 555–562.

Ball, J. T. (1988), An analysis of stomatal conductance, Ph.D. thesis, 89 pp., Stanford Univ., Stanford, Calif.

Berry, J. A. (1988), Studies of mechanisms affecting the fractionation of carbon isotopes in photosynthesis, in *Stable Isotopes in Ecological Research*, edited by P. W. Rundel, pp. 82–94, Springer-Verlag, New York.

Berry, S. C., G. T. Varney, and L. B. Flanagan (1997), Leaf $\delta^{13}C$ in Pinos resinosa trees and understory plants: Variation associated with light and CO_2 gradients, *Oecologia*, *109*, 499–506.

Bonan, G. B. (1996), A land surface model (LSM version 1.0) for ecological, hydrological, and atmospheric studies: Technical description and user's guide, *NCAR/TN-417+STR*, Natl. Cent. for Atmos. Res., Boulder, Colo.

Bonan, G. B. (1998), The land surface climatology of the NCAR Land Surface Model coupled to the NCAR Community Climate Model, *J. Clim.*, *11*, 1307–1326.

Bousquet, P., P. Ciais, P. Peylin, M. Ramonet, and P. Monfray (1999a), Inverse modeling of annual atmospheric CO_2 sources and sinks: 1. Method and control inversion, *J. Geophys. Res.*, *104*, 26,161–26,178.

Bousquet, P., P. Ciais, P. Peylin, M. Ramonet, and P. Monfray (1999b), Inverse modeling of annual atmospheric CO_2 sources and sinks: 2. Sensitivity study, *J. Geophys. Res.*, *104*, 26,179–26,193.

Bowling, D. R., P. P. Tans, and R. K. Monson (2001), Partitioning net ecosystem carbon exchange with isotopic fluxes of CO_2, *Global Change Biol.*, *7*, 127–145.

Bowling, D. R., N. G. McDowell, B. J. Bond, B. E. Law, and J. R. Ehleringer (2002), ^{13}C content of ecosystem respiration is linked to precipitation and vapor pressure deficit, *Oecologia*, *131*, 113–124.

Brugnoli, E., and G. D. Farquhar (2000), Photosynthetic fractionation of carbon isotopes, in *Photosynthesis: Physiology and Metabolism*, edited by R. C. Leegood, T. D. Sharkey, and S. von Caemmerer, pp. 399–434, Kluwer Acad., Norwell, Mass.

Buchmann, N., J. M. Guehl, T. S. Barigah, and J. R. Ehleringer (1997a), Interseasonal comparison of CO_2 concentrations, isotopic composition, and carbon dynamics in an Amazonian rainforest (French Guiana), *Oecolgia*, *110*, 120–131.

Buchmann, N., W.-Y. Kao, and J. R. Ehleringer (1997b), Influence of stand structure on carbon-13 of vegetation, soils, and canopy air within deciduous and evergreen forests in Utah, United States, *Oecologia*, *110*, 109–119.

Ciais, P., P. P. Tans, M. Trolier, J. W. C. White, and R. J. Francey (1995a), A large Northern Hemisphere terrestrial sink induced by the $^{13}C/^{12}C$ ratio of atmospheric CO_2, *Science*, *269*, 1098–1102.

Ciais, P., P. P. Tans, J. W. C. White, M. Trolier, R. J. Francey, J. A. Berry, D. R. Randall, P. J. Sellers, J. G. Collatz, and D. S. Schimel (1995b), Partitioning of ocean and land uptake of CO_2 as inferred by $\delta^{13}C$ measurements from the NOAA Climate Monitoring and Diagnostics Laboratory Global Air Sampling Network, *J. Geophys. Res.*, *100*, 5051–5070.

Ciais, P., P. Friedlingstein, D. S. Schimel, and P. P. Tans (1999), A global calculation of $\delta^{13}C$ of soil respired carbon: Implications for the biospheric uptake of anthropogenic CO_2, *Global Biogeochem. Cycles*, *13*, 519–530.

Collatz, G. J., J. T. Ball, C. Grivet, and J. A. Berry (1991), Physiological and environmental regulation of stomatal conductance, photosynthesis,

and transpiration: A model that includes a laminar boundary layer, *Agric. For. Meteorol.*, *54*, 107–136.

Collatz, G. J., M. Ribas-Carbo, and J. A. Berry (1992), Coupled photosynthesis-stomatal conductance model for leaves of C4 plants, *Aust. J. Plant Physiol.*, *19*, 519–538.

Collatz, G. J., J. A. Berry, and J. S. Clark (1998), Effects of climate and atmospheric CO_2 partial pressure on the global distribution of C-4 grasses: Present, past, and future, *Oecologia*, *114*, 441–454.

Condon, A. G., R. A. Richards, and G. D. Farquhar (1993), Relationship between carbon isotope discrimination, water use efficiency and transpiration efficiency for dryland wheat, *Aust. J. Agric. Res.*, *44*, 1693–1711.

Craig, H. (1953), The geochemistry of stable carbon isotopes, *Geochim. Cosmochim. Acta*, *3*, 53–92.

Craig, H. (1957), Isotopic standards for carbon and oxygen and correction factors for mass-spectrometric analysis of carbon dioxide, *Geochim. Cosmochim. Acta*, *12*, 133–149.

DeFries, R. S., and J. R. G. Townshend (1994), NDVI-derived land-cover classifications at global scale, *Int. J. Remote Sens.*, *15*, 3567–3586.

DeFries, R., M. Hansen, J. R. G. Townshend, and R. Sohlberg (1998), Global land cover classifications at 8 km spatial resolution: The use of training data derived from Landsat imagery in decision tree classifiers, *Int. J. Remote Sens.*, *19*, 3141–3168.

DeFries, R. S., J. R. G. Townshend, and M. C. Hansen (1999a), Continuous fields of vegetation characteristics at the global scale at 1-km resolution, *J. Geophys. Res.*, *104*, 16,911–16,923.

DeFries, R., M. Hansen, J. R. G. Townshend, A. C. Janetos, and T. R. Loveland (1999b), A new global 1 km data set of percent tree cover derived from remote sensing, *Global Change Biol.*, *6*, 247–254.

DeFries, R. S., M. C. Hansen, and J. R. G. Townshend (2000), Global continuous fields of vegetation characteristics: A linear mixture model applied to multiyear 8 km AVHRR data, *Int. J. Remote Sens.*, *21*, 1389–1414.

Denning, A. S., J. G. Collatz, C. Zhang, D. A. Randall, J. A. Berry, P. J. Sellers, G. D. Colello, and D. A. Dazlich (1996a), Simulations of terrestrial carbon metabolism and atmospheric CO_2 in a general circulation model: 1. Surface carbon fluxes, *Tellus, Ser. B*, *48*, 521–542.

Denning, A. S., D. A. Randall, G. J. Collatz, and P. J. Sellers (1996b), Simulations of terrestrial carbon metabolism and atmospheric CO_2 in a general circulation model: 2. Spatial and temporal variations of atmospheric CO_2, *Tellus, Ser. B*, *48*, 543–567.

Denning, A. S., M. E. Nicholls, L. Prihodko, P.-L. Vidale, I. Baker, K. Davis, and P. Bakwin (2003), Simulated and observed variations in atmospheric carbon dioxide over a Wisconsin forest using a coupled ecosystem-atmosphere model, *Global Change Biol.*, *9*, 1241–1250.

Ehleringer, J. R., T. E. Cerling, and B. R. Heliker (1997), C-4 photosynthesis, atmospheric CO_2 and climate, *Oecologia*, *112*, 285–299.

Ekblad, A., and P. Högberg (2001), Natural abundance of ^{13}C in CO_2 respired from forest soils reveals speed of link between tree photosynthesis and root respiration, *Oecologia*, *127*, 305–308.

Enting, I. G., C. M. Trudinger, and R. J. Francey (1995), A synthesis inversion of the concentration and $\delta^{13}C$ of atmospheric CO_2, *Tellus, Ser. B*, *47*, 35–52.

Evans, J. R., and F. Loretto (2000), Acquisition and diffusion of CO_2 in higher plant leaves, in *Photosynthesis: Physiology and Metabolism*, edited by R. C. Leegood, T. D. Sharkey, and S. von Caemmerer, pp. 321–351, Kluwer Acad., Norwell, Mass.

Farquhar, G. D. (1983), On the nature of carbon isotope discrimination in C4 species, *Aust. J. Plant Physiol.*, *10*, 205–226.

Farquhar, G. D., and R. A. Richards (1984), Isotopic composition of plant carbon correlates with water-use efficiency of wheat genotypes, *Aust., J. Plant. Physiol.*, *11*, 539–552.

Farquhar, G. D., S. von Caemmerer, and J. A. Berry (1980), A biochemical model of photosynthetic CO_2 assimilation in C_3 plants, *Planta*, *149*, 78–90.

Farquhar, G. D., M. H. O'Leary, and J. A. Berry (1982), On the relationship between carbon isotope discrimination and the intercellular carbon dioxide concentration in leaves, *Aust. J. Plant Physiol.*, *9*, 121–137.

Farquhar, G. D., K. T. Hubick, A. G. Condon, and R. A. Richards (1988), Carbon isotope discrimination and plant water use efficiency, in *Stable Isotopes in Ecological Research*, edited by P. W. Rundel et al., pp. 21–40, Academic, San Diego, Calif.

Farquhar, G. D., J. R. Ehleringer, and K. T. Hubick (1989), Carbon isotope discrimination and photosynthesis, *Ann. Rev. Plant Physiol. Plant Mol. Biol.*, *40*, 503–537.

Food and Agriculture Organization (1998), *FAO Production Yearbook*, vol. 52, pp. 59–178, Rome.

Francey, R. J. (1985), Cape Grim isotope measurements—A preliminary assessment, *J. Atmos. Chem.*, *3*, 247–260.

Francey, R. J., P. P. Tans, C. E. Allison, I. G. Enting, J. W. C. White, and M. Trolier (1995), Changes in oceanic and terrestrial carbon uptake since 1982, *Nature*, *373*, 326–330.

Francey, R. J., C. E. Allison, D. M. Etheridge, C. M. Trudinger, I. G. Enting, M. Leuenberger, R. L. Langenfelds, E. Michel, and L. P. Steele (1999), A 1000-year high precision record of $\delta^{13}C$ in atmospheric CO_2, *Tellus, Ser. B*, *51*, 170–193.

Friedlingstein, P. C., C. Delire, J. F. Muller, and J. C. Gerard (1992), The climate-induced variation on the continental biosphere: A model simulation of the Last Glacial Maximum, *Geophys. Res. Lett.*, *19*, 897–900.

Fung, I., et al. (1997), Carbon-13 exchanges between the atmosphere and biosphere, *Global Biogeochem. Cycles*, *11*, 507–533.

Gibson, J. K., S. Uppala, P. Kallberg, M. Fiorino, A. Hernandez, K. Onogi, and X. Li (1999), ECMWF 40-year reanalysis (ERA-40)—Archive plans, report, Eur. Cent. for Medium-Range Weather Forecasts, Reading, UK.

Hall, A. E., A. M. Ismail, and C. M. Menendez (1993), Implications for plant breeding of genotypic and drought induced differences in water use efficiency, carbon isotope discrimination and gas exchange, in *Stable Isotopes and Plant Carbon-Water Relations*, edited by J. R. Ehleringer, A. E. Hall, and G. D. Farquhar, pp. 19–28, Academic, San Diego, Calif.

Högberg, P., A. Nordgren, N. Buchmann, A. F. S. Taylor, A. Ekbland, M. N. Högberg, G. Nyberg, M. Ottososn-Löfvenius, and D. J. Read (2001), Large-scale forest girdling shows that current photosynthesis drives soil respiration, *Nature*, *411*, 789–792.

Intergovernmental Panel on Climate Change (2001), *Climate Change 2001: The Scientific Basis. Contribution of Working Group I to the Third Assessment Report of the Intergovernmental Panel on Climate Change*, edited by J. T. Houghton et al., 881 pp., Cambridge Univ. Press, New York.

Kaplan, J. O., I. C. Prentice, and N. Buchmann (2002), The stable carbon isotope composition of the terrestrial biosphere: Modeling at scales from the leaf to the globe, *Global Biogeochem. Cycles*, *16*(4), 1060, doi:10.1029/2001GB001403.

Keeling, C. D. (1958), The concentration and isotopic abundances of atmospheric carbon dioxide in rural areas, *Geochim. Cosmochim. Acta*, *13*, 322–334.

Keeling, C. D. (1961), A mechanism for cyclic enrichment of carbon-12 by terrestrial plants, *Geochim. Cosmochim. Acta*, *24*, 299–313.

Keeling, C. D., R. B. Bacastow, A. F. Carter, S. C. Piper, T. P. Whorf, M. Heiman, W. G. Mook, and H. Roeloffzen (1989), A three-dimensional model of CO_2 transport based on observed winds: 1. Analysis of observational data, in *Aspects of Climate Variability in the Pacific and Western Americas*, *Geophys. Monogr. Ser.*, vol. 55, edited by D. H. Peterson, pp. 165–236, AGU, Washington, D. C.

Keeling, C. D., T. P. Whorf, M. Whalen, and J. van der Plicht (1995), Interannual extremes in the rate of rise of atmospheric CO_2 since 1980, *Nature*, *375*, 666–670.

Leemans, R., and W. Cramer (1991), The IIASA climate database for mean monthly values of temperature, precipitation and cloudiness on a terrestrial grid (RR-9118), report, Int. Inst. for Appl. Syst. Anal., Laxenberg, Austria.

Le Roux, X., T. Bariac, H. Sinoquet, B. Genty, C. Piel, A. Mariotti, C. Girardin, and P. Richard (2001), Spatial distribution of leaf water use efficiency and carbon isotope discrimination within an isolated tree crown, *Plant Cell Environ.*, *24*, 1021–1032.

Lin, G. H., J. R. Ehleringer, P. T. Rygiewicz, M. G. Johnson, and D. T. Tingey (1999), Elevated CO_2 and temperature impacts on different components of soil CO_2 flux in Douglass Fir terracosms, *Global Change Biol.*, *5*, 157–168.

Lloyd, J., and G. D. Farquhar (1994), ^{13}C discrimination during CO_2 assimilation by the terrestrial biosphere, *Oecolgia*, *99*, 201–215.

Lloyd, J., et al. (1996), Vegetation effects on the isotopic composition of atmospheric CO_2 at local and regional scales: Theoretical aspects and a comparison between rain forest in Amazonia and a boreal forest in Siberia, *Aust. J. Plant. Physiol.*, *23*, 371–399.

Lloyd, J., et al. (1997), An alternative interpretation of the appropriateness and correct means for the evaluation of CO_2 recycling indices, *Aust. J. Plant. Physiol.*, *24*, 399–405.

Los, S. O. (1998), Linkages between global vegetation and climate: An analysis based on NOAA advanced very high resolution radiometer data, report, NASA Goddard Space Flight Cent., Greenbelt, Md.

Los, S. O., G. J. Collatz, P. J. Sellers, C. M. Malmstrom, N. H. Pollack, R. S. DeFries, C. J. Tucker, L. Bounoua, and D. A. Dazlich (2000), A global 9-year biophysical landsurface dataset from NOAA AVHRR data, *J. Hydrometeorol.*, *1*, 183–199.

Miller, J. B., P. P. Tans, J. W. C. White, T. J. Conway, and B. W. Vaughn (2003), The atmospheric signal of terrestrial isotopic discrimination and its implication for partitioning of carbon fluxes, *Tellus, Ser. B*, *55*, 197–206.

Mook, W. G., J. G. Bommerson, and W. H. Staverman (1974), Carbon isotope fractionation between dissolved bicarbonate and gaseous carbon dioxide, *Earth Planet. Sci. Lett.*, *22*, 169–176.

Nicholls, M. E., A. S. Denning, L. Prihodko, P.-L. Vidale, I. Baker, K. Davis, and P. Bakwin (2004), A multiple-scale simulation of variations in atmospheric carbon dioxide using a coupled biosphere-atmosphere model, *Journal Geophys. Res.*, *109*, D18117, doi:10.1029/2003JD004482.

O'Leary, M. H. (1981), Carbon isotope fractionation in plants, *Phytochemistry*, *20*, 553–567.

O'Leary, M. H. (1984), Measurement of the isotopic fractionation associated with diffusion of carbon dioxide in aqueous solution, *J. Phys. Chem.*, *88*, 823–825.

O'Leary, M. H. (1993), Biochemical basis of carbon isotope fractionation in plants, in *Stable Isotopes and Plant Carbon Water Relations*, edited by J. R. Ehleringer, A. E. Hall, and G. D. Farquhar, pp. 19–28, Academic, San Diego, Calif.

Ometto, J. P. H. B., L. B. Flanagan, L. A. Martinelli, M. Z. Moreira, N. Higuchi, and J. R. Ehleringer (2002), Carbon isotope discrimination in forest and pasture ecosystems of the Amazon Basin, Brazil, *Global Biogeochem. Cycles*, *16*(4), 1109, doi:10.1029/2001GB001462.

Pataki, D. E., J. R. Ehleringer, L. B. Flanagan, D. Yakir, D. R. Bowling, C. J. Still, N. Buchmann, J. O. Kaplan, and J. A. Berry (2003), The application and interpretation of Keeling plots in terrestrial carbon-cycle research, *Global Biogeochem. Cycles*, *17*(1), 1022, doi:10.1029/2001GB001850.

Ramankutty, N., and J. A. Foley (1998), Characterizing patterns of global land use: An analysis of global croplands data, *Global Biogeochem. Cycles*, *12*(4), 667–686.

Randall, D. A., et al. (1996), A revised land surface parameterization (SiB2) for GCMs: III. The greening of the Colorado State University general circulation model, *J. Clim.*, *9*, 738–763.

Raven, J. A., and G. D. Farquhar (1990), The influence of N metabolism and organic acid synthesis on the natural abundance of isotopes of carbon in plants, *New Phytol.*, *116*, 505–529.

Rayner, P. J., I. G. Enting, R. J. Francey, and R. Langenfelds (1999), Reconstructing the recent carbon cycle from atmospheric CO_2, $\delta^{13}C$ and O_2/N_2 observations, *Tellus, Ser. B*, *51*, 213–232.

Sage, R. F., D. A. Wedin, and M. Li (1999), The biogeography of C4 photosynthesis: Patterns and controlling factors, in *C4 Plant Biology*, edited by R. F. Sage and R. K. Monson, pp. 313–373, Academic, San Diego, Calif.

Saleska, S. R., et al. (2003), Carbon in Amazon forests: Unexpected seasonal fluxes and disturbance-induced losses, *Nature*, *302*, 1554–1557.

Schaefer, K., A. S. Denning, N. Suits, J. Kaduk, I. Baker, S. Los, and L. Prihodko (2002), Effect of interannual variability of the terrestrial CO_2 fluxes, *Global Biogeochem. Cycles*, *16*(4), 1102, doi:10.1029/2002GB001928.

Schleser, G. H., and R. Jayasekera (1985), $\delta^{13}C$ variations of leaves in forests as an indication of reassimilated CO_2 from the soil, *Oecologia*, *65*, 536–542.

Schulze, E.-D., R. Ellis, W. Schulze, P. Trinborn, and H. Ziegler (1996), Diversity, metabolic types and $\delta^{13}C$ carbon isotope ratios in grass flora of Namibia in relation to growth form, precipitation and habitat conditions, *Oecologia*, *106*, 352–369.

Schulze, E.-D., R. J. Williams, G. D. Farquhar, W. Schulze, J. Langridge, J. M. Miller, and B. H. Walker (1998), Carbon and nitrogen isotope discrimination and nitrogen nutrition of trees along a rainfall gradient in northern Australia, *Aust. J. Plant Physiol.*, *25*, 413–425.

Sellers, P. J., Y. Mintz, Y. C. Sud, and A. Dalcher (1986), A simple biosphere model (SiB) for use within general circulation models, *J. Atmos. Sci.*, *43*, 505–531.

Sellers, P. J., D. A. Randall, G. J. Collatz, J. A. Berry, C. B. Field, D. A. Dazlich, C. Zhang, G. D. Collelo, and L. Bounoua (1996a), A revised land surface parameterization (SiB2) for atmospheric GCMs: I. Model formulation, *J. Clim.*, *9*, 676–705.

Sellers, P. J., S. O. Los, C. J. Tucker, C. O. Justice, D. A. Dazlich, G. J. Collatz, and D. A. Randall (1996b), A revised land surface parameterization (SiB2) for atmospheric GCMs: II. The generation of global fields of terrestrial biophysical parameters from satellite data, *J. Clim.*, *9*, 706–737.

Sellers, P. J., et al. (1996c), The ISLSCP initiative I global datasets: Surface boundary conditions and atmospheric forcings for land-atmosphere studies, *Bull. Am. Meteorol. Soc.*, *77*, 1987–2005.

Sternberg, L. D. S. L. (1989), A model to estimate carbon dioxide recycling in forests using $^{13}C/^{12}C$ ratios and concentrations of ambient carbon dioxide, *Agric. For. Meteorol.*, *48*, 163–173.

Sternberg, L. D. S. L., M. Z. Moreira, L. A. Martinelli, R. L. Victoria, E. M. Barbosa, L. C. M. Bonates, and D. C. Nepstad (1997), Carbon dioxide recycling in two Amazonian tropical forests, *Agric. For. Meteorol.*, *88*, 259–268.

Still, C. J., J. A. Berry, G. J. Collatz, and R. S. DeFries (2003), Global distributions of C4 photosynthesis, *Global Biogeochem. Cycles*, *17*(1), 1006, doi:10.1029/2001GB001807.

Tans, P., J. A. Berry, and R. F. Keeling (1993), Oceanic ^{13}C data: A new window on CO_2 uptake by the oceans, *Global Biogeochem. Cycles*, *7*, 353–368.

Tian, H. J., J. M. Melilo, D. W. Kicklighter, A. D. McGuire, J. V. K. Helfrich, B. Moore, and C. J. Vorosmarty (1998), Effect of interannual climate change on carbon storage in Amazonian ecosystems, *Nature*, *396*, 664–667.

Wilson, M. F., and A. Henderson-Sellers (1985), A global archive of land-cover and soils data for use in general circulation climate models, *J. Clim.*, *5*, 119–143.

Yakir, D., and X. F. Wang (1996), Fluxes of CO_2 and water fluxes between terrestrial vegetation and the atmosphere estimated from isotope measurements, *Nature*, *380*, 515–517.

Zobler, L. (1986), A world soil file for global climate modeling, *NASA Tech. Memo.*, *87802*, 32 pp.

I. T. Baker, A. S. Denning, and N. S. Suits, Department of Atmospheric Sciences, Colorado State University, Fort Collins, CO 80523, USA. (nsuits@atmos. colostate.edu)

J. A. Berry, Department of Plant Biology, Carnegie Institution of Washington, Stanford University, 260 Panama Street, Stanford, CA 94305, USA.

J. Kaduk, Department of Geography, University of Leicester, Leicester LE1 7RH, England, UK.

J. B. Miller, NOAA/CMDL, Boulder, CO 80303, USA.

C. J. Still, Geography Department, University of California, Santa Barbara, Santa Barbara, CA 93106-4060, USA.

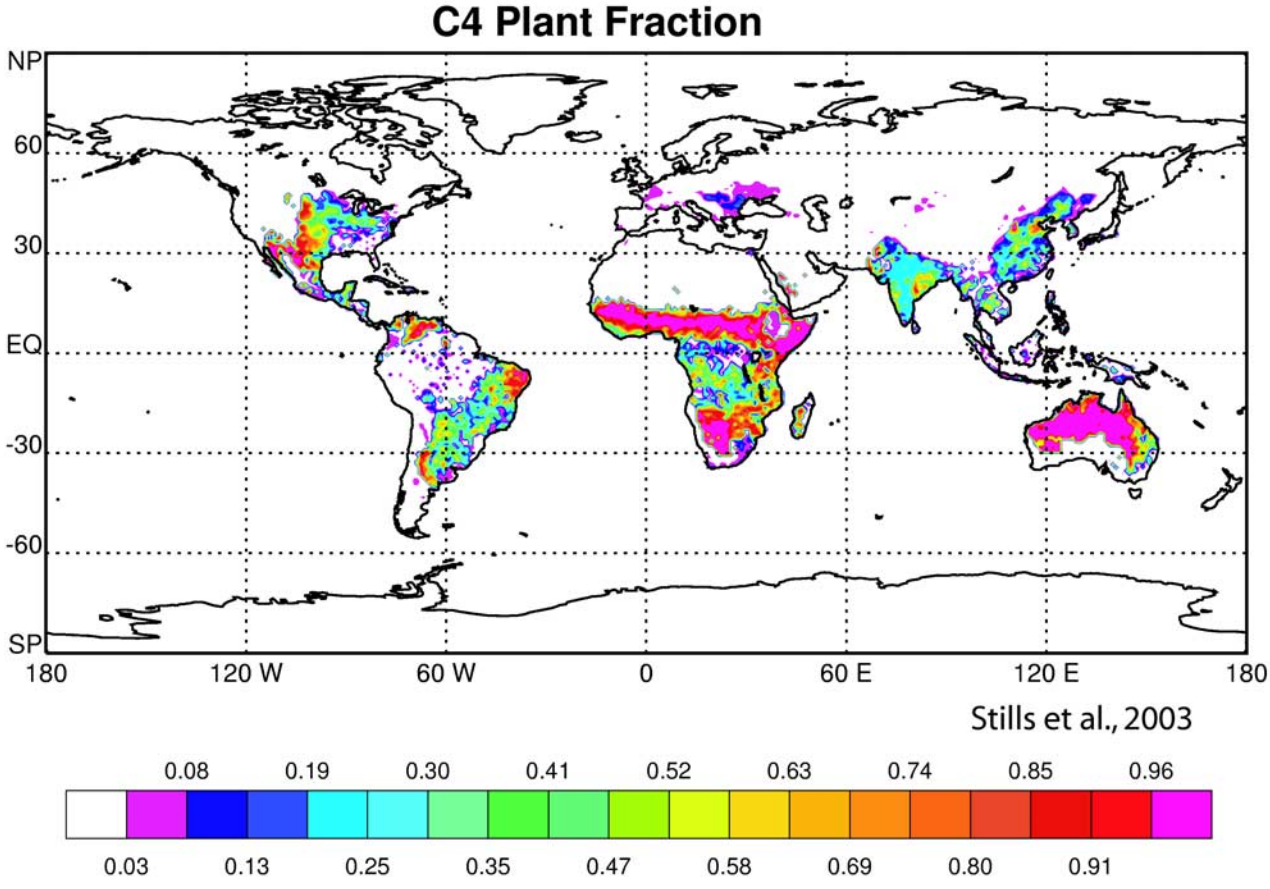

Figure 2. Distribution of C3 and C4 plants [*Still et al.*, 2003] is determined using remote sensing products [*Defries and Townshend*, 1994; *DeFries et al.*, 1998, 1999a, 1999b, 2000], physiological modeling [*Collatz et al.*, 1998], crop fraction maps [*Ramankutty and Foley*, 1998], and areal coverage data on crop types [*FAO*, 1998].

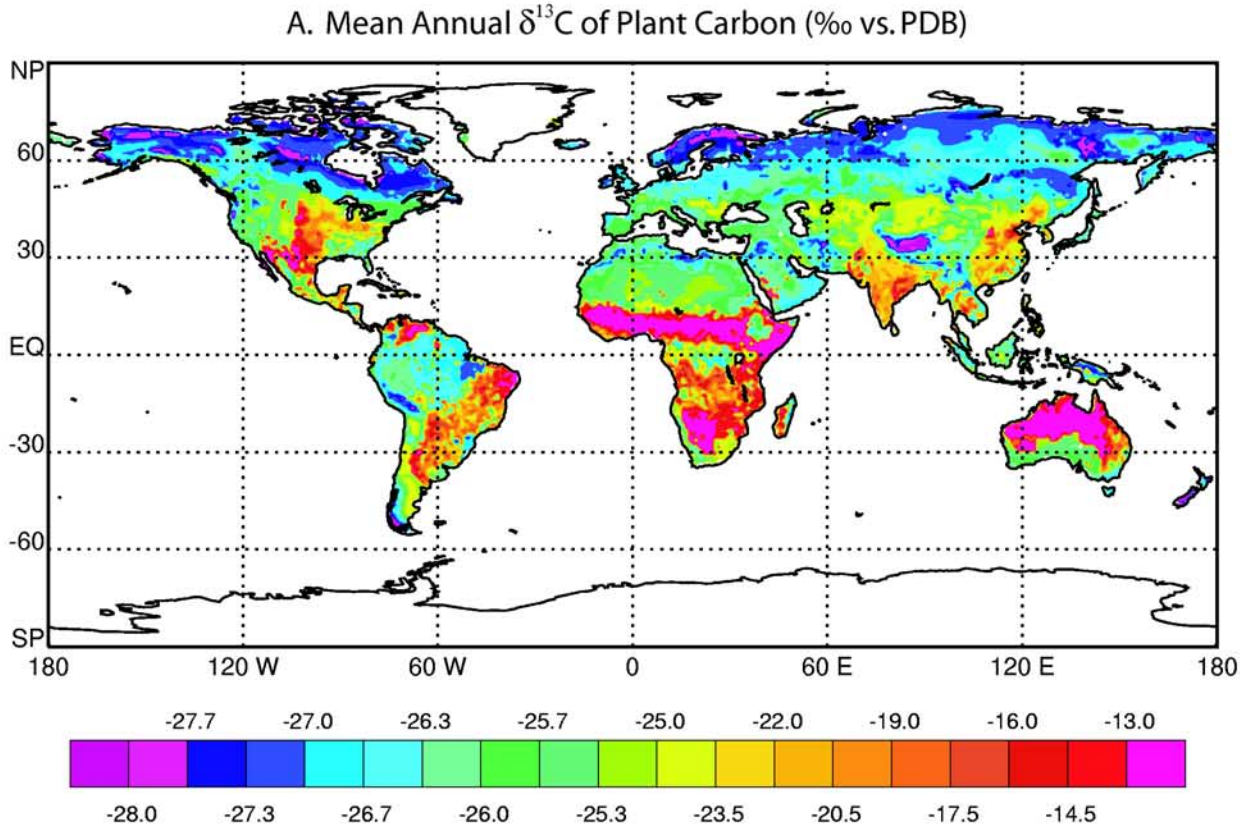
A. Mean Annual δ13C of Plant Carbon (‰ vs. PDB)
NP
60
30
EQ
-30
-60
SP
180
120 W
60 W
0
60 E
120 E
180
-27.7
-27.0
-26.3
-25.7
-25.0
-22.0
-19.0
-16.0
-13.0
-28.0
-27.3
-26.7
-26.0
-25.3
-23.5
-20.5
-17.5
-14.5

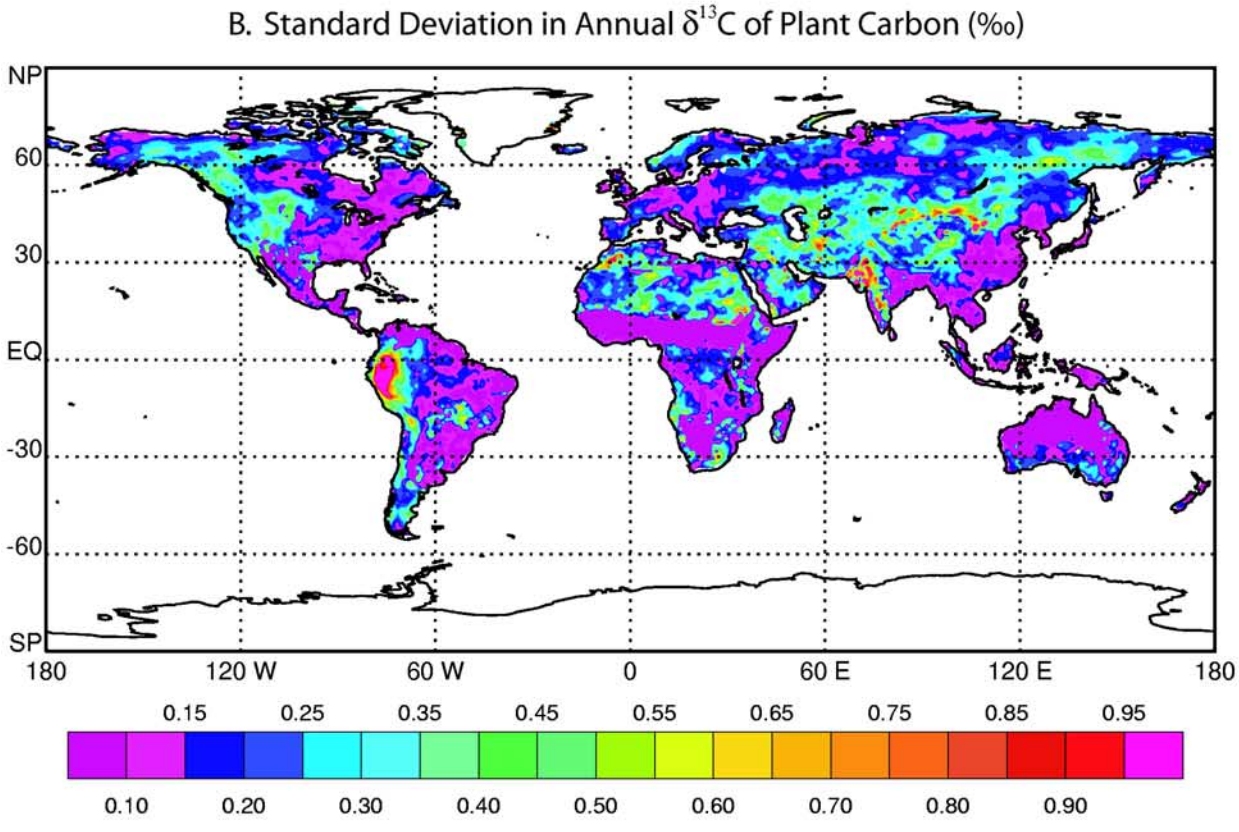
B. Standard Deviation in Annual δ13C of Plant Carbon (‰)
NP
60
30
EQ
-30
-60
SP
180
120 W
60 W
0
60 E
120 E
180
0.15
0.25
0.35
0.45
0.55
0.65
0.75
0.85
0.95
0.10
0.20
0.30
0.40
0.50
0.60
0.70
0.80
0.90

Figure 4

Figure 4. (a) Mean annual assimilation-weighted $\delta^{13}C$ of terrestrial plant carbon from an 11-year simulation (1983–1993) and (b) standard deviation in annual $\delta^{13}C$ values. During each time step, net assimilation is multiplied by the $\delta^{13}C$ of assimilated plant carbon. At the end of the year, the sum of net assimilation times $\delta^{13}C$ is divided by total annual net assimilation to give the $\delta^{13}C$ value of carbon assimilated in each grid cell during that calendar year. The mean is the average of the 11 annual values. The standard deviation is also for those 11 values. Please note the higher resolution used in reporting more negative mean values (Figure 4a). This is done in order to highlight spatial variations in C3 discrimination. There is tremendous spatial variability in $\delta^{13}C$ values of terrestrial carbon. The sharpest spatial contrasts are the result of differences in C3/C4 ratios. Variation in $\delta^{13}C$ values of C3 plants is largely driven by differences in relative humidity during the growing season. Larger than average standard deviations are found in areas where ECMWF predicts significant variations in annual precipitation.

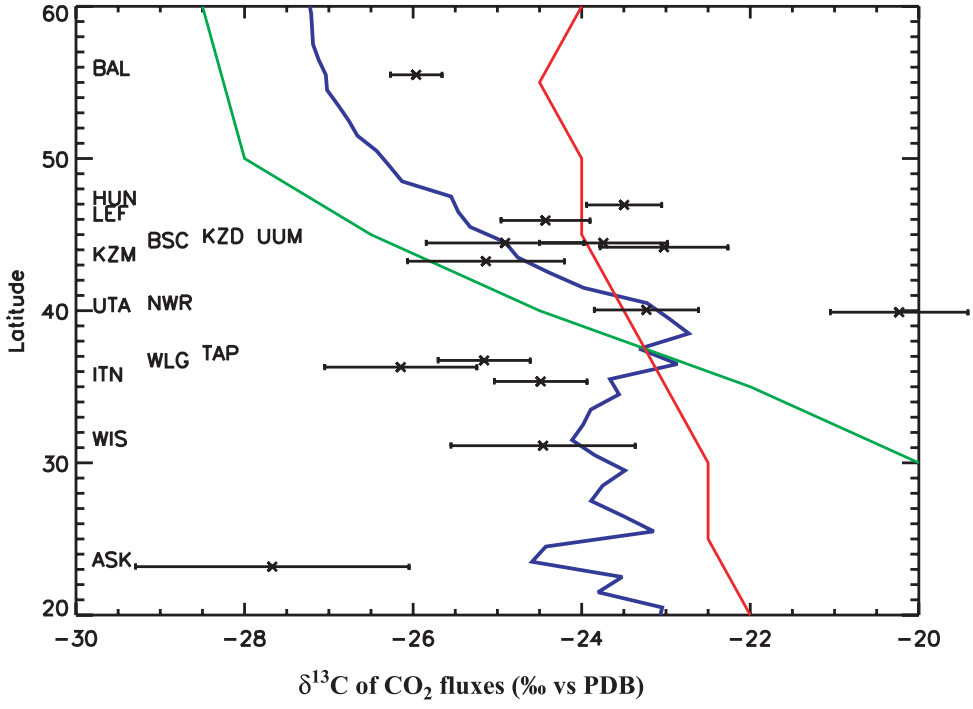

Figure 8. Zonal $\delta^{13}C$ ratios of terrestrial biosphere from *Miller et al.* [2003] (data points with error bars), *Lloyd and Farquhar* [1994] (red line), *Fung et al.* [1997] (green line), and this study (blue line).